PHYSICAL REVIEW B VOLUME 26, NUMBER 6 15 SEPTEMBER 1982

Surface photoeffect in small spheres

David R. Penn and R. W. Rendell*
Electron Physics Group, National Bureau of Standards, Washington, D. C. 20234
(Received 4 December 1981)

A new method is developed to calculate the photoabsorption and photoyield of small spheres. Numerical results are presented for the case of free-electron spheres for photon energies below the plasmon energies. It is found that the excitation of electron-hole pairs due to the presence of the surface results in enhancements in photoabsorption and photoyields that are typically $10-10^2$ relative to the classical results, which only include the excitation of transverse modes. Furthermore, enhancements of the order $10-10^2$ are found in the photoyield of small spheres relative to plane surfaces. These results are consistent with recent experimental results on a number of non-free-electron materials.

I. INTRODUCTION

In recent years the spatial variation of the photon field at a metal surface has been identified as an important element in photoemission experiments.[1–5] This variation is associated with the excitation of plasmons and electron-hole (e-h) pairs by p-polarized incident light; the presence of the surface breaks the symmetry and provides a momentum source for the excitations. There has been a parallel theoretical effort[6–17] to the experimental one. This work has progressed from inclusion of surface plasmons via an additional boundary condition[16] to the unified treatment of plasmon and e-h —pair excitations assuming an infinite surface barrier[6–11] to the use of a realistic surface potential.[11–17] All theoretical work has been restricted to free-electron metals.

Most studies have focused on plane surfaces, however, small particles [e.g. (15—50)-Å radii] are of interest in a number of contexts, particularly in atmospheric physics.[18–20] Recent experiments by Schmitt-Ott, Schurtenberger, and Siegmann[21] (SSS) have focused attention on the unusual optical properties of such particles. They find that the photoyields at threshold of small particles of Ag, Au, MoO_3, and WO_3 are much larger ($\sim 10-10^2$) than the yields from large radii cylinders of the same materials. More precisely, at threshold the yields obey the Fowler-Nordheim relation $Y=c(\hbar\omega-\theta)^2$, where $\hbar\omega$ is the photon energy, θ the work function, and c is a constant. SSS find that c for the sphere is much larger than the c for the large radius cylinder (which may be thought of as a plane surface). The wide variety of materials which show the enhanced yield suggests that the enhancement may be related to e-h —pair excitations rather than plasmons, and it is our purpose to investigate this possibility on the basis of a free-electron model for the sphere. Non-free-electron models are left for the future. Most theoretical work on small spheres has concentrated on the static polarizability[21–23] or on plasmon excitations.[24–29] The present work is the first to focus on the contribution of e-h —pair excitations to the frequency-dependent absorption and yield for a sphere.

In a classic work, Mie[30] treated the transverse modes of the sphere. Ruppin[29] more recently included plasmon excitation in the spirit of Melnyk and Harrison[16] for a plane surface via an additional boundary condition. We treat e-h —pair excitations on an equal footing with plasmon excitations. The reason that e-h —pair excitations are much more important in the case of a sphere than for a plane surface (or large radius cylinder) is as follows. In the absence of e-h —pair excitations a sphere exhibits a sharp peak in adsorption at a frequency $\omega=\omega_p/\sqrt{3}$, where ω_p is the plasmon frequency.[30] The adsorption peak is due to excitation of a surface-plasmon-like mode. If e-h —pair excitations are taken into account, the system can respond off resonance as well as at $\omega_p/\sqrt{3}$. Thus there is a large enhancement in the adsorption well away from ω_p relative to the Mie case of transverse modes only. In the case of a plane it is well known that the surface plasmon at $\omega_p/\sqrt{2}$ cannot be excited by incident light, and consequently inclusion of e-h pairs has little effect on the adsorption.

The key element of our treatment is the use of

 ©1982 The American Physical Society

the *bulk* response function and the simulation of the effects of the surface by a fictitious surface current as discussed in Sec. IV. It will be demonstrated that this approach reproduces the quantum mechanical results of Kliewer and Fuchs[6,7,11] and of Melnyk and Harrison[16] for the plane surface and of Mie[30] and Ruppin[29] for the sphere, and this approach allows inclusion of *e-h*—pair effects in the optical absorption and yield for the first time. A brief description of our work has already been reported.[31]

In Sec. II, we derive formulas for the absorption and yield and show that they depend primarily on the self-consistent determination of the electric and magnetic fields. In Sec. III, we review a number of previous calculations of the fields for both plane surfaces and spheres. In Sec. IV, we introduce our method for calculating the fields in a sphere including the effects of *e-h*—pair production and demonstrate that the method exactly reproduces the results of Kliewer and Fuchs[6,7,11] for a plane surface. In Sec. V, the method is applied to the case of a sphere, formulas for the yield and absorption are given, and it is pointed out that these results reduce to those of Mie[30] and Ruppin[29] in the appropriate limits. In Sec. VI, numerical results are presented and the cases of the sphere and plane surface are compared.

II. THEORY FOR THE ABSORPTION AND YIELD

In order to calculate the absorption and the yield, it is necessary to know the rate at which energy is absorbed by the solid. From a classical point of view this is simply given by the Poynting vector,

$$R_a(\vec{r})=(c/8\pi)\,\mathrm{Re}\{\vec{\nabla}\cdot[\vec{E}(\vec{r})\times\vec{H}(\vec{r})^*]\}\ , \tag{2.1}$$

where R_a is the rate of energy absorption per unit volume and $\vec{E},\vec{H}$ are the electric and magnetic fields. It is useful to derive Eq. (2.1) from quantum mechanics where the rate for absorption by the entire solid is given by the golden rule,

$$R=\frac{2\pi}{\hbar}\sum_{i,j} f_i(1-f_j)\,|M_{ij}|^2 \times\delta(\epsilon_i+\hbar\omega_p-\epsilon_j)\ , \tag{2.2a}$$

where $\hbar\omega_p$ is the photon energy and

$$M_{ij}=\frac{e}{2mc}\int d^3r\,\Psi_i^*(r)(\vec{A}\cdot\vec{P}+\vec{P}\cdot\vec{A})\Psi_j(\vec{r})\ . \tag{2.2b}$$

In Eq. (2.2b), $\vec{A}$ is the total vector potential in the Coulomb gauge in which the electric potential is zero and $\vec{P}=-i\hbar\vec{\nabla}$. Integrating the term involving $\vec{P}\cdot\vec{A}$ in (2.2b) by parts yields

$$M_{ij}=(e/c)\int d^3r\,\vec{A}(r)\cdot\vec{j}_{ij}(\vec{r})\ , \tag{2.3a}$$

where

$$\vec{j}_{ij}(\vec{r})\equiv(\hbar/2im)(\Psi_i^*\nabla\Psi_j-\Psi_j\vec{\nabla}\Psi_i^*)\ . \tag{2.3b}$$

Writing

$$\delta(\chi)=\frac{1}{\pi}\mathrm{Re}\left[\frac{i}{\chi-i\delta}\right] \tag{2.4}$$

and using Eq. (2.3a) and Eq. (2.4) in Eq. (2.2a) gives

$$R=-\frac{2\omega}{\hbar c^2}\,\mathrm{Re}\int d^3r\,d^3r'\vec{A}(\vec{r})\cdot\overleftrightarrow{\sigma}(\vec{r},\vec{r}\,')\cdot\vec{A}(\vec{r}\,')^*\ , \tag{2.5a}$$

where the conductivity tensor, $\overleftrightarrow{\sigma}$, is given by

$$\overleftrightarrow{\sigma}(\vec{r},\vec{r}\,')=-(ie^2/\omega)\sum_{ij}\frac{f_i(1-f_j)}{\epsilon_j-\epsilon_i-\hbar\omega_p+i\delta}\times\vec{j}_{ij}(\vec{r})\,\vec{j}_{ji}(r')^*\ . \tag{2.5b}$$

Use of

$$\vec{E}=-(1/c)\dot{\vec{A}}=i(\omega/c)\vec{A} \tag{2.6}$$

in Eq. (2.5a) yields

$$R=(2/\hbar c)\,\mathrm{Im}\int d^3r\,\vec{A}(\vec{r})\cdot\vec{j}(\vec{r})\ , \tag{2.7}$$

where $\vec{j}$ is the total current given by

$$\vec{j}(\vec{r})=\int d^3r'\overleftrightarrow{\sigma}(\vec{r},\vec{r}\,')\cdot\vec{E}(\vec{r}\,')\ . \tag{2.8}$$

Use of Eq. (2.6) and Maxwell's equations gives

$$\vec{A}\cdot\vec{j}=\frac{c}{i\omega}\vec{\nabla}\cdot(\vec{E}\times\vec{H}^*)+\frac{1}{2i\omega}\frac{\partial}{\partial t}(|\vec{E}|^2+|\vec{H}|^2)\ . \tag{2.9}$$

The time average of the second term on the right-hand side (rhs) of Eq. (2.8) is zero because $\vec{E},\vec{H}\propto\cos(\omega t)$, and use of Eq. (2.9) in (2.7) yields

$$R=\int d^3r\,\mathrm{Re}[(c/8\pi)\vec{\nabla}\cdot(\vec{E}\times\vec{H}^*)]\ . \tag{2.10}$$

Therefore the classical expression for $R_a(\vec{r})$, Eq. (2.1), is in agreement with the quantum mechanical one in the sense of Eq. (2.10); i.e., if the quantum mechanical expression of the absorption per unit volume is taken as the integral of Eq. (2.10). The optical absorption is the absorption per incident photon and is given by

$$\alpha = R/I_0 \ , \tag{2.11}$$

where I_0 is the incident photon flux.

The reason for identifying an expression that gives the absorption per unit volume rather than a total absorption is that we wish to also calculate a yield which is given by

$$Y = \int d^3r \, R_a(\vec{r}) P_t(\vec{r}) P_{es}(\vec{r}) / I_0 \ , \tag{2.12}$$

where R_a is the rate that photons are absorbed at a point $\vec{r}$, $P_t(\vec{r})$ is the probability an electron photoexcited at point $\vec{r}$ reaches the surface, and $P_{es}(\vec{r})$ is the probability it escapes. We are interested in calculating the yield at threshold so P_t represents the probability that the photoexcited electron reaches the surface without any inelastic scattering.

Before turning to the calculation of $R_a(\vec{r})$, we will deal with $P_t P_{es}$ in Eq. (2.12). These quantities, which measure the probability that a photoexcited electron actually contributes to the threshold yield, will differ for a plane surface and a sphere. The calculation for the case of a plane surface is as follows. The energy of a photoexcited electron may be written as

$$\epsilon_k = (\hbar^2/2m)(k_{\parallel}^2 + k_{\perp}^2) \ , \tag{2.13}$$

where $k_{\perp}$ is the momentum of the electron in a direction normal to the surface. The electron will escape from the solid if it has a normal energy greater than the work function ϕ, i.e.,

$$\hbar\omega_p + (\hbar^2/2m)k_{\perp}^2 \geq \epsilon_F + \phi \ , \tag{2.14}$$

where ϵ_F is the Fermi energy. The probability that the electron gets to the surface without inelastic scattering is

$$P_t = e^{-d/\lambda} = e^{-(z/\lambda)[1+(k_{\parallel}/k_{\perp})^2]^{1/2}} \ , \tag{2.15}$$

where d is the distance the electron must travel to reach the surface assuming a straight trajectory and motion in the direction $\vec{k} = (k_{\parallel}, k_{\perp})$, λ is the mean free path, and z is the shortest distance between the point of photoexcitation and the surface. Let $P(z)$ be the probability that an electron photoexcited a distance z from the surface escapes without scattering. Use of Eqs. (2.14) and (2.15) gives

$$P(z) = (2\pi/N) \int_{k_F(1-\Delta)^{1/2}}^{k_F} dk_{\perp} \int_0^{(k_F^2 - k_{\perp}^2)^{1/2}} dk_{\parallel} k_{\parallel} e^{-(z/\lambda)[1+(k_{\parallel}/k_{\perp})^2]^{1/2}} \ , \tag{2.16}$$

where k_F is the Fermi momentum and $N = (4\pi/3)k_F^3$, and

$$\Delta = (\hbar\omega_p - \phi)/\epsilon_F \ . \tag{2.17}$$

Equation (2.16) assumes that the excited electrons have a homogeneous momentum distribution. We are interested in $P(z)$ at threshold, i.e., for $\Delta \ll 1$ in which case

$$P_t(z) P_{es}(z) \simeq \tfrac{3}{16} \Delta^2 e^{-z/\lambda} \ . \tag{2.18}$$

We next discuss the corresponding calculation for a sphere. Consider the probability of escape without scattering for an electron photoexcited at $\vec{r}$ where the origin is chosen to be the center of the sphere. The electron moves towards the surface with a momentum $\vec{k}$, and the component of momentum normal to the surface is

$$k_{\perp} = k(1 - \bar{r} + \bar{r}^2 \mu^2)^{1/2} \ , \tag{2.19}$$

where $\bar{r} = r/R$, $\mu = \hat{k} \cdot \hat{r} = \cos\theta_R$, and R is the sphere radius. The condition for escape is from Eqs. (2.14) and (2.17),

$$k_{\perp} > k_F \sqrt{1 - \Delta} \ . \tag{2.20}$$

The distance the electron travels in reaching the surface is

$$d = d(r, \theta_R) = R\{\bar{r}\mu + [1 + \bar{r}^2(\mu^2 - 1)]^{1/2}\} \ , \tag{2.21}$$

and the probability an electron photoexcited at r escapes without scattering is

$$P(r) = (2\pi/N) \int_{-1}^{1} d\mu \int_{k_F\gamma}^{k_F} dk \, k^2 e^{-d(r,\mu)/\lambda} \tag{2.22a}$$

where

$$\gamma = \sqrt{1 - \Delta} / [1 + \bar{r}^2(\mu^2 - 1)]^{1/2} \ . \tag{2.22b}$$

At threshold $\Delta \ll 1$ and $d(r,\mu)$ can be replaced by its value at $\mu = 1$ for $\mu > 0$ and by its value at $\mu = -1$ for $\mu < 0$ so that

$$P_t(r)P_{es}(r) \to (e^{-(R-r)/\lambda}+e^{-(R+r)/\lambda})(2\pi/N)\int \frac{d\mu}{[1-(\Delta/\bar{r}^2)]^{1/2}}\int_{k_F\gamma}^{k_F} dk\, k^2$$
$$=(e^{-(R-r)/\lambda}+e^{-(R+r)/\lambda})\tfrac{3}{16}(\Delta/\bar{r})^2 . \tag{2.23}$$

The reason for the rather singular behavior of Eq. (2.23) at $\bar{r}=0$ is that at threshold only electrons traveling normal to the sphere can escape and all electrons originating at $\bar{r}=0$ satisfy that condition.

It is now useful to compare the yields of a plane surface and a sphere at threshold assuming a constant excitation rate $R_a(\vec{r})=\bar{R}_a$. The yields are given by

$$Y=\left[\frac{\bar{R}_a}{I_0}\right]\int d^3r\, P_t P_{es} . \tag{2.24}$$

Use of Eq. (2.18) for P_tP_{es} and $I_0=(c/8\pi)E_0^2 S$, where E_0 is the amplitude of the incident light and S is the surface area of the plane, gives the yield for the plane

$$Y_p=a\bar{R}_a\tfrac{3}{16}\Delta^2\lambda , \tag{2.25}$$

where $a=1/[(c/8\pi)E_0^2]$. Use of Eq. (2.23) and $I_0=(c/8\pi)E_0^2\pi R^2$ gives the sphere yield as

$$Y_s=a\bar{R}_a\tfrac{3}{4}\Delta^2\lambda(1-e^{-2R/\lambda}) . \tag{2.26}$$

Thus,

$$Y_s/Y_p=4(1-e^{-2R/\lambda}) , \tag{2.27}$$

and $0<Y_s/Y_p<4$ for $0<R/\lambda<\infty$. For $\lambda \gg R$ the plane surface has the larger yield since photon absorption takes place over a length λ in the plane and a length R in the sphere. The main point is that if R_a is constant the sphere yield cannot be more than 4 times the plane yield.

III. REVIEW OF CALCULATIONS OF $\vec{E},\vec{H}$ FOR THE PLANE AND THE SPHERE

We now review calculations of $\vec{E}$ and $\vec{H}$ for a plane and a sphere that (1) treat excitations of transverse modes only (this yields the Fresnel equations for a plane and Mie theory for a sphere) and (2) include plasmons plus transverse modes.

Maxwell's equations may be written in their microscopic form as (for $\mu=1$)

$$\vec{\nabla}\times\vec{E}+(1/c)\dot{\vec{H}}=0 , \tag{3.1a}$$

$$\vec{\nabla}\times\vec{H}-(1/c)\dot{\vec{E}}=4\pi/cj , \tag{3.1b}$$

$$\vec{\nabla}\cdot\vec{E}=4\pi\rho , \tag{3.1c}$$

$$\vec{\nabla}\cdot\vec{H}=0 , \tag{3.1d}$$

where $\vec{j}$ and ρ are the total current and charge density. In the gauge where the scalar potential is zero,

$$\vec{E}=-(1/c)\dot{\vec{A}} , \tag{3.2a}$$

$$\vec{H}=\vec{\nabla}\times\vec{A} , \tag{3.2b}$$

where $\vec{A}$ is the vector potential. From Eq. (3.1) and (3.2), $\vec{A}$ satisfies

$$\vec{\nabla}\times\vec{\nabla}\times\vec{A}-\left[\frac{\omega}{c}\right]^2\vec{A}=\frac{4\pi}{c}\vec{j} , \tag{3.3}$$

where it has been assumed that $\vec{A}\sim\vec{A}(\vec{r})e^{-i\omega t}$. The current $\vec{j}$ and the vector potential $\vec{A}$ are related via the dielectric tensor $\overleftrightarrow{\epsilon}=\overleftrightarrow{\epsilon}(\vec{r},\vec{r}';\omega)$ by the equation[11]

$$\frac{4\pi}{c}\vec{j}(\vec{r})=-\left[\frac{\omega}{c}\right]^2\vec{A}(\vec{r})+\left[\frac{\omega}{c}\right]^2\int d^3r'\,\overleftrightarrow{\epsilon}(\vec{r},\vec{r}')\cdot\vec{A}(\vec{r}') . \tag{3.4}$$

Use of Eq. (3.4) in (3.3) gives

$$\vec{\nabla}\times\vec{\nabla}\times\vec{A}-\left[\frac{\omega}{c}\right]^2\overleftrightarrow{\epsilon}\cdot\vec{A}=0 , \tag{3.5a}$$

where

$$\overleftrightarrow{\epsilon}\cdot\vec{A}=\int d^3r'\,\overleftrightarrow{\epsilon}(\vec{r},\vec{r}')\cdot\vec{A}(\vec{r}') . \tag{3.5b}$$

In order to determine $\vec{E},\vec{H}$ in the solid given an incident photon field, it is necessary to apply the boundary conditions satisfied by the fields. These are derived from Eqs. (3.1a) and (3.1b) in the usual way[31] and give

$$\vec{E}_{||}\text{ continuous} , \tag{3.6a}$$

$$\vec{H}_{||}\text{ continuous} , \tag{3.6b}$$

where the derivation assumes that $\vec{E},\vec{H}$ and $\vec{j}$ are not singular at the boundary. However an additional boundary condition can be derived from Eq. (3.1c). Constructing a pill box across the solid surface in the usual way[32] and integrating Eq. (3.1c) over the volume of the box V_1 gives

$$\int_{V_1} dV\, \vec{\nabla}\cdot\vec{E}=4\pi\int_{V_1} dV\rho\ . \tag{3.7}$$

Letting the width of the pill box shrink yields

$$\int_{V_1} dV\, \vec{\nabla}\cdot\vec{E}=0\ , \tag{3.8}$$

as long as the charge density is finite. Use of Green's theorem gives

$$\int_{S_1} d\vec{S}\cdot\vec{E}=0\ , \tag{3.9}$$

where the integral is over the surface of the pill box. Equation (3.9) implies

$$\vec{E}_\perp \text{ continuous} \tag{3.10}$$

and this condition has been discussed in detail by Melnyk and Harrison.[16] The boundary condition Eq. (3.10) has traditionally been overlooked; however, it has validity equal to that of Eq. (3.6b) which rests on the assumption that the current j is well behaved while Eq. (3.10) depends on ρ being well behaved. j and ρ are related by the equation of continuity

$$\vec{\nabla}\cdot\vec{j}=-\dot{\rho}\ , \tag{3.11}$$

so the two conditions are not independent. The excitation of plasmons by p-polarized light is a direct consequence of Eq. (3.1c) and that effect was also overlooked for many years.

In an infinite media $\overleftrightarrow{\epsilon}=\overleftrightarrow{\epsilon}(\vec{r}-\vec{r}\,')$, and Eq. (3.5a) can be Fourier transformed to give

$$\vec{k}\times\vec{k}\times\vec{A}(\vec{k})-\left[\frac{\omega}{c}\right]^2\overleftrightarrow{\epsilon}^B(\vec{k})\cdot\vec{A}(\vec{k})=0\ , \tag{3.12}$$

where $\vec{A}(\vec{k})$ is the Fourier transform of $\vec{A}(\vec{r})$ and $\overleftrightarrow{\epsilon}^B$ is the Fourier transform of the bulk dielectric tensor. The Fresnel equations for a semi-infinite plane surface are derived by assuming that in the solid $\vec{A}$ satisfies Eq. (3.12), where $\overleftrightarrow{\epsilon}^B=\overleftrightarrow{\epsilon}_t(k,\omega)$ and $\overleftrightarrow{\epsilon}_t$ is the transverse dielectric tensor which is usually taken to have its $k=0$ value. Equation (3.12) has the solution

$$\vec{A}_B(\vec{r})=\hat{\epsilon}_k A_B e^{i\vec{k}\cdot\vec{r}}\ , \tag{3.13a}$$

with k determined by

$$k^2-\left[\frac{\omega}{c}\right]^2\epsilon_t(0)=0\ , \tag{3.13b}$$

and

$$\hat{\epsilon}_k\cdot\vec{k}=0\ . \tag{3.13c}$$

The A vector outside the plane surface represents the incoming and scattered light

$$\vec{A}_0=\hat{\epsilon}_0 A_0 e^{i\vec{k}_0\cdot\vec{r}}+\hat{\epsilon}_s A_s e^{-i\vec{k}_s\cdot\vec{r}}\ , \tag{3.14a}$$

where

$$k_0^2=k_s^2=\left[\frac{\omega}{c}\right]^2 \tag{3.14b}$$

and

$$\hat{\epsilon}_0\cdot\vec{k}_0=0,\ \ \hat{\epsilon}_s\cdot\vec{k}_s=0\ . \tag{3.14c}$$

The amplitudes A_s, A_B are determined by the use of the boundary conditions (3.6). Thus the Fresnel equations are derived by assuming that Maxwell's equation in the semi-infinite solid can be replaced by those in the bulk and that only transverse excitations need be considered. This latter condition should be relaxed as discussed by Melnyk and Harrison[16]; it is now well known that p-polarized light incident on a plane surface can create plasmons. This effect can be treated[16] using Eq. (3.14) by assuming $\overleftrightarrow{\epsilon}^B$ includes a longitudinal response as well as a transverse one. Equation (3.12) then implies that[16]

$$\vec{A}_B=\hat{\epsilon}_k A_t^B e^{i\vec{k}\cdot\vec{r}}+\hat{q}A_l^B e^{i\vec{q}\cdot\vec{r}}\ , \tag{3.15a}$$

where $\vec{k}$ and $\vec{q}$ satisfy

$$k^2-\left[\frac{\omega}{c}\right]^2\epsilon_t(k,\omega)=0\ , \tag{3.15b}$$

and

$$\epsilon_l(q,\omega)=0\ , \tag{3.15c}$$

where ϵ_l is the longitudinal dielectric function. The $\vec{A}$ vector outside the solid is still given by Eq. (3.14). The presence of the longitudinal wave in Eq. (3.15a) means that an extra boundary condition is required to determine A_l^B, and this condition is given by Eq. (3.10). The creation of plasmons is only important for photon energies ω where Eq. (3.15c) can be satisfied; however, even for $\omega<\omega_p$ Eq. (3.15c) has solutions with complex q.

We next review Mie theory,[30,32] the excitation of transverse modes in a sphere by an incident photon beam. The theory makes use of a basis set which is written in spherical coordinates. The basis vectors are denoted by $\vec{m}_i$ and $\vec{n}_i$ where i represents a set of quantum numbers to be defined and $\vec{m}_i, \vec{n}_i$ satisfy

$$\vec{\nabla}\times\vec{\nabla}\times\vec{C}-k^2\vec{C}=0\ , \tag{3.16}$$

$$\vec{\nabla}\cdot\vec{C}=0\ , \tag{3.17}$$

where $\vec{C}$ represents any of the $\vec{m}_i,\vec{n}_i$. In order to find $\vec{m},\vec{n}$, it is convenient to define an auxiliary vector $\vec{l}$ which satisfies

$$\vec{\nabla}\times\vec{l}=0\ , \tag{3.18}$$

so that

$$\vec{l}=\vec{\nabla}\psi\ . \tag{3.19}$$

A condition is now imposed on ψ,

$$\nabla^2\psi+k^2\psi=0\ , \tag{3.20}$$

which implies that $\vec{l}$ satisfies

$$\vec{\nabla}\vec{\nabla}\cdot\vec{l}+k^2\vec{l}=0\ . \tag{3.21}$$

It is now straightforward[32] to show that if

$$\vec{m}=\vec{\nabla}\times(r\psi)=-\vec{r}\times\vec{l}$$
$$=(1/k)\vec{\nabla}\times\vec{n}\ , \tag{3.22a}$$

and

$$\vec{n}=(1/k)\vec{\nabla}\times\vec{m}\ , \tag{3.22b}$$

then $\vec{m},\vec{n}$ satisfies Eqs. (3.16) and (3.17). Thus a solution of Eq. (3.20) yields $\vec{m},\vec{n}$. The solution of (3.20) is

$$\psi_{lm\substack{e\\o}}=z_n(kr)Y^m_{l,\substack{e\\o}}(\theta,\phi)\ , \tag{3.23a}$$

$$Y^m_{l,\substack{e\\o}}(\theta,\theta)=P_{lm}(\cos\theta)\times\begin{Bmatrix}\cos\\ \sin\end{Bmatrix}m\phi\ , \tag{3.23b}$$

where z_n is a spherical Bessel function, Y is an even or odd real spherical harmonic, and P_l^m is a Legendre polynomial.

In Mie theory, it is assumed that the dielectric tensor $\overleftrightarrow{\epsilon}$ in Eq. (3.14) is the bulk *local* transverse dielectric response so that $\vec{A}$ satisfies Eqs. (3.16) and (3.17) with

$$k^2=\left[\frac{\omega}{c}\right]^2\epsilon_t(0,\omega)\ . \tag{3.24}$$

Consequently, if one writes

$$\vec{A}_B=\sum_i(a_i\vec{m}_i+b_i\vec{n}_i)\ , \tag{3.25}$$

where $\vec{A}_B$ represents the vector potential in the sphere, then $\vec{A}_B$ will satisfy the wave equation (3.16) because $\vec{m}_i,\vec{n}_i$ do, and $\vec{A}_B$ will be transverse since $\vec{m}_i,\vec{n}_i$ are. Furthermore, $\vec{m}_i,\vec{n}_i$ are expressed in spherical coordinates[32] so the boundary conditions, $\vec{E}_{||},\vec{H}_{||}$ continuous can be applied. A convenient way of writing the $\vec{m},\vec{n}$ and $\vec{l}$ is

$$\vec{m}_{lm\substack{e\\o}}(k,\vec{r})=-ij_l(k\vec{r})\vec{L}Y_{lm\substack{e\\o}}\ , \tag{3.26a}$$

$$\vec{n}_{lm\substack{e\\o}}(k,\vec{r})=\frac{l(l+1)}{kr}j_l(kr)Y_{lm\substack{e\\o}}\hat{r}$$
$$-i\frac{[krj_l(kr)]'}{kr}\hat{r}\times\vec{L}Y_{lm\substack{e\\o}}\ , \tag{3.26b}$$

$$\vec{l}_{lm\substack{e\\o}}(k,\vec{r})=kj_l'(kr)Y_{lm\substack{e\\o}}\hat{r}$$
$$-ik\frac{j_l(kr)}{kr}\hat{r}\times\vec{L}Y_{lm\substack{e\\o}}\ , \tag{3.26c}$$

where

$$\vec{L}=-i\vec{r}\times\vec{\nabla}\ , \tag{3.26d}$$

and the prime denotes differentiation with respect to kr. In the sphere $\vec{A}_B$ must be well behaved so $z_l(kr)=j_l(kr)$, a spherical Bessel function of the first kind.

The coefficients a_i,b_i in Eq. (3.25) are obtained by solving the boundary value problem; the incoming plane wave is expressed as[31]

$$\vec{A}_i=A_i\sum_{l=0}^{\infty}i^l\frac{2l+1}{l(l+1)}[\,m_{l1o}(\vec{r},k_0)$$
$$-i\vec{n}_{l1e}(\vec{r},k_0)]\ , \tag{3.27}$$

where $k_0^2=(\omega/c)^2$, and the z_l entering (3.27) is a Bessel function of the first kind while that entering reflected wave $\vec{A}_r$ is an outgoing Hankel function;

$$\vec{A}_r=\sum_{l=1}^{\infty}\frac{i^l(2l+1)}{l(l+1)}(d_l\vec{m}_{l1o}-ie_l\vec{n}_{l1e})\ . \tag{3.28}$$

The boundary conditions $\vec{E}_{||},\vec{H}_{||}$ continuous are used to determine a_i, b_i, d_i, and e_i in terms of A_0.

The optical absorption as a function of ω in the limit k_0R, $k_tR\ll 1$ predicted by Mie theory for a free-electron metal is shown in Fig. 1. There is a large peak in the absorption at $\omega_p/\sqrt{3}$ that can be easily understood from electrostatics. In the $k_0\to 0$ limit, the incident electric field, $E_0\hat{x}e^{ik_0z}$, reduces to $E_0\hat{x}$, a constant field, and the corresponding electric field in the sphere is[31]

$$E_B=3E_0/(\epsilon+2)\ , \tag{3.29}$$

where ϵ is the dielectric function at $k=0$,

$$\epsilon=1-\frac{\omega_p^2}{\omega(\omega+i/\tau)}\ , \tag{3.30}$$

where τ is a relaxation time. Equations (3.29) and (3.30) show that E_B peaks at $\omega \simeq \omega_p/\sqrt{3}$.

Mie theory for a sphere was extended by Ruppin[29] to include longitudinal excitations in the form of plasmons by noting that in the long-wavelength limit the vector potential that describes plasmons satisfies

$$\vec{\nabla}\vec{\nabla}\cdot\vec{A}_{pl}+q^2\vec{A}_{pl}=0 , \tag{3.31a}$$

$$\vec{\nabla}\times\vec{A}_{pl}=0 , \tag{3.31b}$$

where the plasmon wave vector q is related to ω by

$$\omega=\omega_p+\gamma q^2 \tag{3.31c}$$

and γ is material dependent. Equations (3.31) are satisfied by the $\vec{1}_i$ defined in Eqs. (3.18)–(3.21), and thus $\vec{A}_{pl}$ can be expanded in the $\vec{1}_i$ and the total vector potential in the sphere has the form

$$\vec{A}_B=\sum_i[a_i\vec{m}_i(\vec{r},k)+b_i\vec{n}_i(\vec{r},k)+c_i\vec{1}_i(\vec{r},q)] , \tag{3.37}$$

where k satisfies Eq. (3.24). The vector potential outside the sphere has the same form as before, $\vec{A}=\vec{A}_i+\vec{A}_r$ with $\vec{A}_i,\vec{A}_r$ given by Eqs. (3.27) and (3.28). There is now an additional coefficient c_i and so the additional boundary condition, $\vec{E}_\perp$ continuous, must be used.

The optical absorption α for a free-electron small sphere including plasmon excitations is determined by Ruppin.[29] The peak at $\omega_p/\sqrt{3}$ is shifted slightly and there are peaks in α. The peaks result when the excited plasmons have a wavelength q which satisfy a geometric resonance condition; i.e., when ω, the frequency of the incident light, is such that the plasmon wave vector given by Eq. (3.31c) satisfies a resonant condition. These resonances are very similar to those that occur in a thin film[7] when $q_\perp a=n\pi$ where $q_\perp$ is the component of the plasmon wave vector perpendicular to the film, a is the thickness of the film and n is an odd integer.

IV. THEORY OF SURFACE-INDUCED ABSORPTION

The theories we have reviewed thus far assume that the vector potential in the solid is determined by the vector potential in an infinite media. Thus the dielectric tensor $\overleftrightarrow{\epsilon}$ is replaced by that appropriate to the bulk and surface effects are included only via the boundary conditions. Absorption is then due to excitation of transverse modes, plasmons, and in the case of non-free-electron metals, interband transitions, but surface-induced e-h –pair production is neglected. This effect has been discussed in detail for the case of a plane surface and a free-electron solid[6–16] and we now study the case of a free-electron sphere. To this end we make the ansatz that the vector potential of a finite solid is determined by that of an infinite solid with a current located at the actual surface. That is, the vector potential of the solid satisfies

$$\vec{\nabla}\times\vec{\nabla}\times\vec{A}-\left[\frac{\omega}{c}\right]^2\overleftrightarrow{\epsilon}_B\cdot\vec{A}=\vec{J} , \tag{4.1}$$

where $\overleftrightarrow{\epsilon}_B$ is the *bulk* dielectric tensor and $\vec{J}$ is a general current located at the surface of the solid. The role of this fictitious surface current is to simulate the scattering of electrons from the surface. $\vec{J}$ and $\vec{A}$ will be determined by the boundary conditions $\vec{E}_{||}$, $\vec{H}_{||}$, and $\vec{E}_\perp$ continuous. It will be shown that the ansatz, Eq. (4.1), exactly reproduces the quantum mechanical results of Kliewer and Fuchs[6,7,11] for the case of a plane surface if $\overleftrightarrow{\epsilon}_B$ is taken to be the Lindhard dielectric tensor.[33] If the longitudinal response function is the hydrodynamic one rather than that of Lindhard the results of Melnyk and Harrison[16] are obtained. For a sphere, use of the hydrodynamic response in Eq. (4.1) will be shown to yield the results of Ruppin,[29] and Mie theory[30] follows if the longitudinal response is neglected altogether. Thus the ansatz, Eq. (4.1), is capable of reproducing a large number of previous results despite the absence of a fundamental justification.

There are actually two different ways that the ansatz of Eq. (4.1) can be interpreted. The first is to let $\vec{J}$ be a general current confined to the surface of the solid; $\vec{J}$ will have two components parallel to the surface of the solid and one normal to the surface. The second possibility is to restrict $\vec{J}$ to being a surface current without a component normal to the surface. In this case, it would appear that the three boundary conditions will overdetermine $\vec{A}$; however, a solution of

$$\vec{\nabla}\times\vec{\nabla}\times\vec{A}-\left[\frac{\omega}{c}\right]^2\overleftrightarrow{\epsilon}_B\cdot\vec{A}=0 \tag{4.2}$$

can be added to the field $\vec{A}$ obtained from Eq. (4.1). In particular, we add the solution for the transverse field $\vec{A}_t$ obtained from Eq. (4.2) which satisfies

$$\vec{\nabla}\times\vec{\nabla}\times\vec{A}_t-k^2\vec{A}_t=0\ , \tag{4.3}$$

where k^2 is given by Eq. (3.15b).

The two different forms of the ansatz give identical results for a number of different cases; they both reproduce the results of Kliewer and Fuchs[6,7,11] for the plane surface and those of Ruppin[29] and Mie[30] as discussed above. The results are not identical for the case of a sphere when *e-h* excitations are taken into account. However, the numerical values for the adsorption predicted by the two treatments are in remarkably close agreement as will be discussed in Sec. VI.

In order to illustrate the use of the ansatz (in both forms), we apply it to the case of a semi-infinite solid. We begin by using Eq. (4.1) to determine the vector potential for the case of a plane wave incident on the plane surface of a free-electron metal and show that Eq. (4.1) gives precisely the results of Kliewer and Fuchs[6,7,11] who carried out a quantum mechanical treatment. It is also significant that the theory of Kliewer and Fuchs[6,7] reproduces that of Melnyk and Harrison[16] in the limit of a hydrodynamic longitudinal response function, i.e., small wave vectors and no *e-h*—pair excitations. For the case of a plane surface located at $z=0$ the general form for the fictitious current $\vec{J}$ is

$$\vec{J}=\delta(z)(j_x\hat{x}+j_y\hat{y}+j_z\hat{z})\ , \tag{4.4}$$

where j_x,j_y,j_z are functions of x and y to be determined from the boundary conditions and hence from the form of the incident light which we write as

$$\vec{A}_0=\hat{e}A_0e^{i(\vec{k}_0\cdot\vec{r}-\omega t)} \tag{4.5}$$

where $\hat{e}$ and $\vec{k}_0$ lie in the xz plane for the case of p polarization and

$$k_0^2=(\omega/c)^2\ . \tag{4.6}$$

The fact that $\vec{k}_0$ lies in the xz plane as well as the boundary conditions imply that the bulk vector potential which satisfies Eq. (4.1) must have the form

$$\vec{A}(\vec{r})=\vec{A}(z)e^{i(kx-\omega t)}\ , \tag{4.7}$$

and the fictitious current, Eq. (4.4), must be of the form

$$j_i(x,y)=\gamma_ie^{i(kx-\omega t)},\quad i=x,y,z \tag{4.8}$$

where γ_i is a constant. Our treatment now follows the formalism of Ref. 11 rather closely.[34] Equation (4.1) written in rectangular coordinates gives

$$-A_x''+ikA_z'-k_0^2B_x=\gamma_x\delta(z)\ , \tag{4.9a}$$

$$ikA_x'+k^2A_z-k_0^2B_z=\gamma_z\delta(z)\ , \tag{4.9b}$$

$$-A_y''+k^2A_y-k_0^2B_y=\gamma_y\delta(z)\ , \tag{4.9c}$$

where the prime denotes differentiation with respect to z and

$$B_i(z)=\sum_{j=x,y}\int_{-\infty}^{\infty}dz'\epsilon_{ij}^B(k,z-z')\times A_j(z'),\quad i=x,z \tag{4.10a}$$

$$B_y(z)=\int_{-\infty}^{\infty}dz'\epsilon_{yy}^B(k,z-z')A_y(z')\ , \tag{4.10b}$$

where $\epsilon_{ij}^B(k,z)$ is the Fourier transform (with respect to x) of the bulk dielectric tensor. Equation (4.9a) can be Fourier transformed with respect to z and solved for A_x,A_y to obtain [Appendix A, Eq. (A5)] the following:

$$A_x(z)=\int_{-\infty}^{\infty}\frac{dp}{2\pi}e^{ipz}\left[\gamma_x\left[\frac{p^2}{q^2g}-\frac{k^2}{k_0^2q^2\epsilon_l}\right]-\gamma_zkp\left[\frac{1}{q^2g}+\frac{1}{k_0^2q^2\epsilon_l}\right]\right]\ , \tag{4.11a}$$

$$A_z(z)=\int_{-\infty}^{\infty}\frac{dp}{2\pi}e^{ipz}\left[-\gamma_xkp\left[\frac{1}{q^2g}+\frac{1}{k_0^2q^2\epsilon_l}\right]+\gamma_z\left[\frac{k^2}{q^2g}-\frac{p^2}{k_0^2q^2\epsilon_l}\right]\right]\ , \tag{4.11b}$$

where

$$q^2=k^2+p^2\ , \tag{4.11c}$$

$$g=q^2-k_0^2\epsilon_t(q)\ , \tag{4.11d}$$

$$\epsilon_l=\epsilon_l(q)\ , \tag{4.11e}$$

and ϵ_t,ϵ_l are the transverse and longitudinal bulk dielectric functions. The wave vector in vacuum has the form, Eq. (A7),

$$A_x^{(0)}(z)=\frac{-p_0A_0(e^{ip_0z}-\rho e^{-ip_0z})}{k_0}\ , \tag{4.12a}$$

$$A_z^{(0)}(z)=\frac{kA_0(e^{ip_0z}+\rho e^{-ip_0z})}{k_0}\ , \tag{4.12b}$$

where

$$p_0^2=k_0^2-k^2\ . \tag{4.12c}$$

Equations (4.12) follow from the equations for the vector potential outside the solid and from Eq. (4.5). Use of the boundary conditions and the approximation $\epsilon_t(q)=\epsilon_t(0)$ yields the results of Eq. (A16),

$$\gamma_y,\gamma_z=0\ , \tag{4.13a}$$

$$\gamma_x=\frac{2p_0k_0A_0}{-i\frac{1}{2}(p_0+p_t)+k^2\int_{-\infty}^{\infty}\frac{dp}{2\pi}\frac{1}{q^2}\left[\frac{1}{\epsilon_l}-1\right]}\ , \tag{4.13b}$$

where

$$p_t^2=k_0^2\epsilon_t(0)-k^2\ . \tag{4.13c}$$

These results agree exactly with those of Kliewer and Fuchs[6,7,11] and demonstrate that the ansatz, Eq. (4.1), is exact within the approximation of specular scattering for the case of a plane surface.

We next use the form of the ansatz in which the current $\vec{J}$ has no component normal to the surface. This means $j_z=0$ in Eq. (4.4) and therefore $\gamma_z=0$ in Eqs. (4.8)–(4.11). However, the particular solution of Eq. (4.3) given by

$$A_x^{(1)}=\frac{-p_tA_1}{q_t}e^{ip_tz}\ , \tag{4.14a}$$

$$A_z^{(1)}=\frac{kA_1}{q_t}e^{ip_tz}\ , \tag{4.14b}$$

is now added to $A_x(z),A_z(z)$ given by Eqs. (4.11a) and (4.11b) [assuming $\epsilon_t(q)=\epsilon_t(0)$]. Use of the three boundary conditions to match $\vec{A}$ to the vacuum solution Eqs. (4.12a) and (4.12b) yields the result $A_i^{(1)}=0$ and Eq. (4.13b) is again obtained.

V. ABSORPTION BY A SPHERICAL METAL PARTICLE

The case of a sphere is now treated using the ansatz of Eq. (4.1). The results include the effects of e-h —pair excitations. It will be shown that if this effect is neglected by approximating the longitudinal dielectric function by the hydrodynamic one, then the results of Ruppin[29] are obtained, and if longitudinal response is neglected altogether, then the results of Mie theory[30] follow. It will also be pointed out that some recent results of Dasgupta and Fuchs[17] may be obtained by altering the form of the fictitious current $\vec{J}$ entering Eq. (4.1).

According to the ansatz of Eq. (4.1), a fictitious surface current is introduced at the surface of the sphere of radius R which separates two regions, each of which is filled by the bulk material and described by the bulk dielectric tensor. Solutions to Eq. (4.1) for $r<R$ are taken to be equal to the vector potential inside the metal particle of the actual problem.

It is convenient to expand the solutions of Eq. (4.1) in terms of the functions $\vec{m}$, $\vec{n}$, and $\vec{l}$ introduced in Eqs. (3.26),

$$\vec{A}(\vec{r})=-(i/k_0)\sum_{l=1}^{\infty}\frac{i^l(2l+1)}{l(l+1)}\int_0^{\infty}dk\,[\,a_l(k)\vec{m}_{l1o}(k,\vec{r})+b_l(k)\vec{n}_{l1e}(k,\vec{r})+c_l(k)\vec{l}_{l1e}(k,\vec{r})]\ , \tag{5.1}$$

where $k_0=\omega/c$, and the specific choices of $m=1$ and even or odd spherical harmonics for the $\vec{m}$, $\vec{n}$, and $\vec{l}$ are determined by the fact that the incident light is linearly polarized, Eq. (3.27). The fields in the metal particle can be excited over a range of wave vectors, k, due to the dispersion of the transverse and longitudinal modes. The absorption is given by

$$\alpha=(1/\pi)\int_{r=R}d\Omega\,\hat{r}\cdot\mathrm{Re}(\vec{E}\times\vec{H}^*)\ , \tag{5.2}$$

where $\vec{E}$ and $\vec{H}$ are determined from $\vec{A}$ by Eq. (3.2). Therefore we need to solve for the coefficients $a_l(k)$, $b_l(k)$, and $c_l(k)$ in (5.1). In terms of the model problem, these are determined by the coupling to the fictitious current in (4.1). In the case that we use the general form of the fictitious current, it can be written in terms of a *general* expansion in vector spherical harmonics on the surface $r=R$:

$$\vec{J}=\frac{-i}{k_0}\delta(r-R)\sum_{l=1}^{\infty}i^l\frac{2l+1}{l(l+1)}(\alpha_l\hat{r}Y_{e1l}+\beta_l\vec{L}Y_{o1l}+\gamma_l\hat{r}\times\vec{L}Y_{e1l})\ , \tag{5.3}$$

where α, β, and γ are constants. This expression for the current is appropriate for the first form of the ansatz. The constants are coupling strengths for the current and they can be related to the field coefficients a, b, and c by an extremely useful theorem which we derive in Appendix B and we state here as

$$\overleftrightarrow{\epsilon}_B\cdot\vec{m}(k,\vec{r})=\epsilon_t(k)\vec{m}(k,\vec{r})\ , \tag{5.4a}$$

$$\overleftrightarrow{\epsilon}_B \cdot \vec{n}(k,\vec{r}) = \epsilon_t(k)\vec{n}(k,\vec{r}) \ , \tag{5.4b}$$

$$\overleftrightarrow{\epsilon}_B \cdot \vec{l}(k,\vec{r}) = \epsilon_l(k)\vec{l}(k,\vec{r}) \ . \tag{5.4c}$$

These relations have many applications for the electrodynamics of particles. Using (5.1) and (5.3) in (4.1), and applying (5.4), we find in Appendix C:

$$a_l(k) = i\frac{8}{c}(kR)^2\beta_l \frac{j_l(kR)}{k^2 - k_0^2\epsilon_t} \ , \tag{5.5a}$$

$$b_l(k) = \frac{8}{c}\{i\gamma_l[kRj_l(kR)]' + \alpha_l j_l(kR)\} \times \frac{kR}{k^2 - k_0^2\epsilon_t} \ , \tag{5.5b}$$

$$c_l(k) = \frac{-8}{c}\{i\gamma_l l(l+1)j_l(kR) + \alpha_l[kRj_l'(kR)]\}\frac{R}{k_0^2\epsilon_l} \ . \tag{5.5c}$$

The coupling constants α, β, and γ for the model problem can be determined by applying the boundary conditions $\vec{E}_{||}$, $\vec{H}_{||}$, and $E_\perp$ continuous at the surface of the particle between the fields of the actual problem. For the actual problem, in addition to the excited field (5.1) within the particle and the incoming field (3.27) outside of the particle, there will be a reflected field outside the particle given by Eq. (3.28). The boundary conditions are now applied to Eq. (3.27) (with $A_i = 1$), Eq. (3.28), and Eq. (5.1). One obtains from $\vec{E}_{||}$ continuous the conditions

$$\int dk\,[a_l(k)j_l(kR)] - d_l h_l(k_0R) = j_l(k_0R) \ , \tag{5.6a}$$

$$i\int dk\left[b_l(k)\left[\frac{kRj_l(kR)}{kR}\right]' + c_l(k)\frac{j_l(kR)}{R}\right] - e_l\frac{1}{k_0R}[k_0Rh_l(k_0R)]' = \frac{1}{k_0R}[k_0Rj_l(k_0R)]' \ , \tag{5.6b}$$

From $\vec{H}_{||}$ continuous one obtains

$$i\int dk\left[\frac{k}{k_0}b_l(k)j_l(kR)\right] - e_l h_l(k_0R) = j_l(k_0R) \ , \tag{5.6c}$$

$$\int dk\{a_l(k)[kRj_l(kR)]'\} - d_l[k_0Rh_l(k_0R)]' = [k_0Rj_l(k_0R)]' \ , \tag{5.6d}$$

and from $\vec{E}_\perp$ continuous,

$$i\int dk\left[b_l(k)\frac{l(l+1)}{kR}j_l(kR) + c_l(k)kj_l'(kR)\right] - e_l\frac{l(l+1)}{k_0R}h_l(k_0R) = \frac{l(l+1)}{k_0R}j_l(k_0R) \ . \tag{5.6e}$$

Here h_l is the Hankel function of the first kind. Equations (5.5) and (5.6) yield equations for the coupling constants α,β,γ, and thus the particle fields by (5.1), (3.27), and (3.28). However, for the case of optical excitation of small metal particles, we can approximate $\epsilon_t(k,\omega)$ by its local form $\epsilon_t(0,\omega)$. It is necessary to operate in the x-ray region in order to produce important structure from the transverse dispersion for the particle sizes considered here. Using a local transverse dielectric function, the contributions to the integrals over wave vector in (5.1) from the denominators involving ϵ_t in (5.5a) and (5.5b) can be done analytically and this simplifies the equations for the coupling constants. In this approximation $\vec{A}(\vec{r})$ can also be explicitly obtained by the use of Eqs. (5.5) in Eq. (5.1):

$$\vec{A}(\vec{r}) = (8\pi R/\omega)\sum_{l=1}^{\infty}\frac{i^l(2l+1)}{l(l+1)}\Bigg[\beta_l k_t R h_l(k_tR)\vec{m}_{l1o}(k_t,\vec{r}) + \{i\gamma_l[k_tRh_l(k_tR)]' + \alpha_l h_l(k_tR)\}\vec{n}_{l1e}(k_t,\vec{r}) - [1/(\pi i k_0^2)]\int dk[i\gamma_l l(l+1)j_l(kR) + \alpha_l kRj_l'(kR)]\vec{l}(k,\vec{r})\left[\frac{1}{\epsilon_l(k)} - \frac{1}{\epsilon_l(o)}\right]\Bigg] \ . \tag{5.7}$$

The contour techniques used in the integrals over k in Eqs. (5.1) and (5.6) and the resolution of ambiguities at $r=R$ that arise from the boundary conditions, Eq. (5.6), are illustrated in Appendix D. Integrals over the longitudinal dielectric function still remain; however, these can be evaluated numerically. The solutions for the coupling constants are found by straightforward, but lengthy, algebra to be given by

$$\alpha_l=-\frac{c}{R}\frac{(l+1)\eta_l}{4\pi h_l(k_0R)\left[1-\frac{2}{\pi}\Delta_l\right]}\,, \tag{5.8a}$$

$$\beta_l=\frac{c}{R}\frac{i}{4\pi k_tRk_0R\Gamma_l}\,, \tag{5.8b}$$

$$\gamma_l=\frac{c}{R}\frac{1}{il}\frac{[1-(l+1)\eta_l]}{4\pi h_l(k_0R)\left[1-\frac{2}{\pi}\Delta_l\right]}\,, \tag{5.8c}$$

where

$$\eta_l=\frac{Q_l^{(2)}-(l+1)Q_l^{(1)}}{Q_l^{(3)}-(l+1)Q_l^{(2)}}\,, \tag{5.8d}$$

$$\Delta_l=\frac{(l+1)(Q_l^{(1)}Q_l^{(3)}-Q_l^{(2)}Q_l^{(2)})}{(l+1)Q_l^{(2)}-Q_l^{(3)}}\,, \tag{5.8e}$$

$$\Gamma_l=h_l(k_0R)[k_tRj_l(k_tR)]'-j_l(k_tR)[k_0Rh_l(k_0R)]'\,, \tag{5.8f}$$

$$Q_l^{(i)}=R\int_0^\infty dq[\epsilon_l^{-1}(q)-1]f_l^{(i)}(qR)\,, \tag{5.8g}$$

$$f_l^{(1)}(\rho)=[j_l(\rho)]^2\,, \tag{5.8h}$$

$$f_l^{(2)}(\rho)=j_l(\rho)\rho j_{l-1}(\rho), f_l^{(3)}(\rho)=[\rho j_{l-1}(\rho)]^2\,, \tag{5.8i}$$

and $k_t^2=k_0^2\epsilon_t(\omega)$ to get

$$f_l^{(2)}(\rho)=j_l(\rho)\rho j_{l-1}(\rho)\,.$$

The expressions for α_l, β_l, and γ_l are now used with (5.1) to evaluate the absorption as given by (5.2). The necessary angular integrals are given in Appendix E, and we find

$$\alpha=\sum_{l=1}^{\infty}\frac{2(2l+1)}{k_0R}\mathrm{Im}\left[|A_l|^2j_l(k_tR)\{[k_tRj_l(k_tR)]'\}^*-|B_l|^2j_l^*(k_tR)[k_tRj_l(k_tR)]'(k_t^*/k_t)-\int_0^\infty dq\,C_l(q)\frac{j_l(qR)}{R}B_l^*k_t^*Rj_l^*(k_tR)\right]. \tag{5.9a}$$

where

$$A_l=4\pi k_tRh_l(k_tR)\frac{R}{c}\beta_l\,, \tag{5.9b}$$

$$B_l=i4\pi\frac{R}{c}\{i\gamma_l[k_tRh_l(k_tR)]'+\alpha_lh_l(k_tR)\}\,, \tag{5.9c}$$

$$C_l(q)=-\frac{8}{k_0^2}[\epsilon_l^{-1}(q)-\epsilon_l^{-1}(0)]\frac{R}{c}[i\gamma_ll(l+1)j_l(qR)+\alpha_lqRj_l'(qR)]\,. \tag{5.9d}$$

The only approximation in (5.9) within our surface current ansatz is the neglect of dispersion for the transverse dielectric constant. The expressions further simplify greatly if retardation can also be neglected. For particles with $R\lesssim 50$ Å excited at optical frequencies, this is certainly the case because $k_0R,k_tR\ll 1$. In this regime the Bessel functions of argument k_0R and k_tR can be expanded to lowest order. When this is done, the first term in the large parentheses of (5.9a) is found to be real and thus the β_l coupling constant of the surface current (5.3) does not contribute to the absorption in this limit. The second and third terms then combine to give a very simple expression

$$\alpha\simeq-2\sum_{l=1}^{\alpha}(k_0R)^{2l-1}[(2l-1)!!]^{-2}\times\mathrm{Im}\left[1-\frac{2}{\pi}\Delta_l^*\right]^{-1}\,, \tag{5.10}$$

where Δ_l is given by (5.8e). For the very small spheres considered in this limit, the $l=1$ term dominates.

In the limit the e-h —pair excitations are neglected but plasmon excitation is allowed by using a plasmon pole dielectric function, it is easily shown (Appendix F) that

$$\Delta_l = -\frac{\pi}{2}\left[\frac{l+1}{2l+1}\right]\left[\frac{1}{\epsilon(0)}-1\right] \times \frac{\rho_0 j_{l-1}(\rho_0)-(2l+1)j_l(\rho_0)}{\rho_0 j_l'(\rho_0)} . \tag{5.11}$$

The absorption obtained by use of Eq. (5.11) in Eq. (5.8) can be shown to be equal to that calculated from the theory of Ruppin.[29]

There is an aspect of this theory that is not entirely satisfactory; there are terms that arise from the boundary conditions (5.6) of the form

$$\lim_{r\to R} \alpha_l \int_0^\infty dk[krj_{l-1}(kr)kRj_{l-1}(kR)]\frac{1}{\epsilon_l(k)} = \alpha_l \int_0^\infty dk[kRj_{l-1}(kR)]^2\left[\frac{1}{\epsilon_l(k)}-1\right] + \lim_{r\to R}\alpha_l \int_0^\infty dk\, krj_{l-1}(kr)kRj_{l-1}(kR) . \tag{5.12}$$

The precise reason this type of term appears in the theory is discussed at the beginning of Appendix D. In the case $l=1$, the second integral on the rhs of Eq. (5.12) is zero for $r<R$ and infinite for $r=R$. For obvious reasons, we have set the integral equal to zero in deriving Eq. (5.9). The singular behavior can be traced directly to the charge density associated with the radial current density; i.e., $\dot{\rho}=-\nabla\cdot\vec{j}$ includes a term proportional to $\alpha_l\partial/\partial r\delta(r-R)$. The second form of the ansatz avoids this problem, although as mentioned earlier both forms yield numerical results that are very similar.

We next calculate the adsorption using the second form of the ansatz; the fictitious surface current has no component normal to the surface so that Eq. (5.3) is replaced by

$$\vec{j}_0 = (-i/k_0)\delta(r-R) \times \sum_{l=1}^\infty \frac{i^l(2l+1)}{l(l+1)}(\beta_l^{(0)}\hat{r}Y_{o1l}+\gamma_l^{(0)}\hat{r}\times\vec{L}Y_{e1l}) . \tag{5.13}$$

The field $\vec{A}_0$ that satisfies Eq. (4.1) (with $\vec{J}$ replaced by $\vec{J}_0$) is given by Eq. (5.1) with a_l,b_l,c_l now denoted by $a_l^{(0)},b_l^{(0)},c_l^{(0)}$. To this field is added a solution of Eq. (4.2),

$$\vec{A}_1(\vec{r}) = -(i/k_0)\sum_{l=1}^\infty \frac{i^l(2l+1)}{l(l+1)}[a_l^{(1)}\vec{m}_{l1o}(k_t,\vec{r}) + b_l^{(1)}\vec{n}_{l1e}(k_t,\vec{r})] , \tag{5.14}$$

where k_t satisfies (3.15b). The quantities $a_l^{(0)},b_l^{(0)},c_l^{(0)}$ are given by Eq. (5.5) with $\alpha_l=0$:

$$a_l^{(0)}(k) = \frac{8}{c}\, i(kR)^2\frac{j_l(kR)}{k^2-k_0^2\epsilon_t}\beta_l^{(0)} , \tag{5.15a}$$

$$b_l^{(0)}(k) = \frac{8}{c}\, i[kRj_l(kR)]'\frac{kR}{k^2-k_0^2\epsilon_t}\gamma_l^{(0)} , \tag{5.15b}$$

$$c_l^{(0)}(k) = \frac{-8}{c}\, il(l+1)j_l(kR)\frac{R}{k_0^2\epsilon_l}\gamma_l^{(0)} . \tag{5.15c}$$

Use of (5.15a) in (5.1) results in a contribution to $\vec{A}_0$ proportional to $\beta_l^{(0)}\vec{m}_{l1o}(k_t,\vec{r})$, exactly the same form as the first term in Eq. (5.14). Consequently, $a_l^{(1)}$ merely serves to redefine $\beta_l^{(0)}$, and one set

$$a_l^{(1)}=0 . \tag{5.16}$$

This in not true for $b_l^{(1)}$ because use of (5.15b) in (5.1) yields two terms, one proportional to $\gamma_l^{(0)}\vec{n}_{l1e}(k_t,\vec{r})$ and a second that comes from the pole at $k=0$.

The boundary conditions are given by Eq. (5.6) with the replacements

$$a_l(k)\to a_l^{(0)}(k) , \tag{5.17a}$$

$$b_l(k)\to b_l^{(0)}(k)+\delta(k-k_t)b_l^{(1)} , \tag{5.17b}$$

$$c_l(k)\to c_l^{(0)}(k) . \tag{5.17c}$$

The boundary conditions together with Eq. (5.15) yield expressions for $\beta_l^{(0)}$, $\gamma_l^{(0)}$, and $b_l^{(1)}$. The quantity $\beta_l^{(0)}$ is equal to β_l of Eq. (5.8b), and

$$\gamma_l^{(0)} = \frac{c}{8R}\frac{1}{h_l(k_0R)}\frac{1}{\lambda_l} , \tag{5.18a}$$

$$\lambda_l = l(l+1)Q_l - \left[\frac{l+1+l\epsilon_t}{1-\epsilon_t}\right]R_l , \tag{5.18b}$$

$$Q_l = R\int_0^\infty dq\, j_l(qR)^2\left[\frac{1}{\epsilon_l(q)}-\frac{1}{\epsilon_t}\right] , \tag{5.18c}$$

$$R_l = R\int_0^\infty dq\, qR^< j_l'(qR^<) \times j_l(qR^>)\left[\frac{1}{\epsilon_l(q)}-\frac{1}{\epsilon_t}\right] , \tag{5.18d}$$

where $\epsilon_t \equiv \epsilon_l(0)$, and for numerical purposes (see Appendix D) it is best to express Q_l and R_l in terms of $Q_l^{(1)}$ and $Q_l^{(2)}$ of Eq. (5.8g):

$$Q_l = Q_l^{(1)} + \frac{\pi}{2}\frac{1}{2l+1}\left[1-\frac{1}{\epsilon_t}\right], \tag{5.19a}$$

$$R_l = Q_l^{(2)} - (l+1)Q_l^{(1)} + \frac{\pi}{2}\frac{l}{2l+1}\left[1-\frac{1}{\epsilon_t}\right]. \tag{5.19b}$$

Also,

$$b_l^{(1)} \equiv -\pi\frac{4R}{c}[k_t R h_l(k_t R)]' \gamma_l^{(1)}, \tag{5.20a}$$

where

$$\gamma_l^{(0)} = -\frac{c}{8R}\frac{1}{h_l(k_0 R)}\frac{1}{\lambda_l}[(R_l/\delta_l)+1], \tag{5.20b}$$

where

$$\delta_l = \frac{i\pi}{2}k_t j_l(k_t R)h_l(k_t R)\left[\frac{1}{\epsilon_t}-1\right]. \tag{5.20c}$$

The adsorption is obtained from Eq. (5.9a) with A_l given by (5.9b) and B_l is replaced by $B_l^{(0)}$, where

$$B_l^{(0)} = 4\pi i\frac{R}{c}[k_t R h_l(k_t R)]'(i\gamma_l^{(0)} + i\gamma_l^{(1)}), \tag{5.21a}$$

and C_l is replaced by $C_l^{(0)}$, where

$$C_l^{(0)}(q) = \frac{-8}{k_0^2}\frac{R}{c}[\epsilon_l^{-1}(q) - \epsilon_t^{-1}] \times l(l+1)j_l(qR)i\gamma_l^{(0)}. \tag{5.21b}$$

In the limit $k_0 R, k_t R \ll 1$, the adsorption is given by

$$\alpha^{(0)} = \frac{2}{|1-\epsilon_t|^2}\sum_l \frac{(l+1)(2l+1)}{[(2l-1)!!]^2}\frac{(k_0 R)^{2l-1}}{|\lambda_l|^2} \times \mathrm{Im}[\epsilon_t |R_l|^2 + lQ_l R_l^*(\epsilon_t - |\epsilon_t|^2)]. \tag{5.22}$$

The $l=1$ term agrees with the result of Ref. 17.

The threshold yield for a sphere is given by Eq. (2.12) with $P_t P_{es}$ given by Eq. (2.23) and R_a given by Eq. (2.1) with $\vec{E},\vec{H}$ determined from the vector potential $\vec{A}$ in the sphere. The yield determined in this way is the threshold yield because $P_t P_{es}$ of Eq. (2.23) are derived by assuming the photon energy is only a little larger than the work function. In the case of a sphere Eq. (2.23) gives $P_t P_{es} \propto (1/r)^2$ due to the semiclassical treatment of the photoexcited electron. In a proper quantum-mechanical treatment the electron would be described by a wave packet. We simply assume now in a small sphere the electron is uniformly distributed and so $P_t P_{es}$ is approximated by its average over the sphere,

$$P_t(r)P_{es}(r) \sim (3\lambda/R)[1-\exp(-2R/\lambda)], \tag{5.23}$$

where λ is the electron mean free path. Thus the yield is given by

$$Y = (3\lambda/R)[1-\exp(-2R/\lambda)]\alpha, \tag{5.24}$$

where α is the absorption of the sphere. This procedure probably underestimates the yield since $R_a(\vec{r})$ is largest in the center of the sphere where $P_t(r)P_{es}(r)$ is largest (if calculated quantum mechanically).

The transverse dielectric function ϵ_t that appears in the various formulas in this section is taken to be

$$\epsilon_t(q,\omega) \simeq \epsilon_t(0,\omega) = 1 - \frac{\omega_p^2}{\omega(\omega + i/\tau)}, \tag{5.25}$$

where τ is a phenomenlogical relaxation time and $\epsilon_l(q,\omega)$ is the Lindhard dielectric function[33] as modified by Mermin[35] to take account of the relaxation time τ. For $q=0$, $\epsilon_l = \epsilon_t$, where ϵ_t is given by Eq. (5.25).

VI. NUMERICAL RESULTS AND DISCUSSION

In Fig. 1, we present results for the adsorption of a sphere as a function of the frequency of the incident light. The curves labeled α_{Mie}, α_{I}, and α_{II} refer to the adsorption calculated by Mie theory, by Eq. (5.10) and Eq. (5.22), respectively. Thus α_{I} refers to the form of the ansatz that includes a component of the fictitious current that is normal to the surface whereas α_{II} does not. The calculations were carried out for a sphere radius of 25 Å, an electron density corresponding to Na ($r_s = 4$),

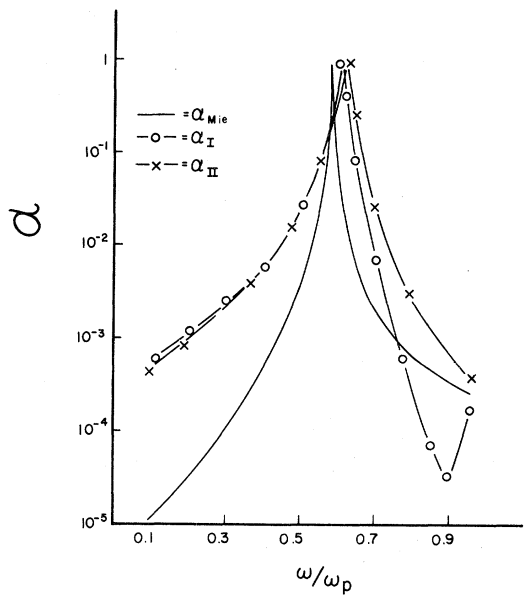

FIG. 1. Plot of the absorption of a sphere with radius $R=25$ Å, electron density $r_s=4$, and scattering time $\omega_p\tau=10^3$. α_{Mie} is the adsorption given by Mie theory and includes only transverse mode excitation. α_{I} and α_{II} include *e-h* excitations as well as plasmons and transverse modes and are calculated from two different forms of the ansatz. They are given by Eqs. (5.10) and (5.22), respectively.

and $\omega_p\tau=10^3$. The adsorption shows no dramatic dependence on R (for $k_0R \ll 1$) or on r_s. The choice $\omega_p\tau=10^3$ is appropriate to weak electron scattering and has been used extensively by Kliewer. It has been pointed out[36] that within the local-field approximation the effect of *e-h* pairs can be incorporated into Mie theory in an approximate way by the use of a relaxation time $\tau=R/v_F$ where v_F is the Fermi velocity. In the case of Fig. 1, this would give $\omega_p\tau\simeq 20$. However, the local-field approximation is clearly invalid if nonlocal effects are taken into account, and thus while the scheme of simulating *e-h* —pair excitation by means of a scattering time $\tau=R/v_F$ is quite physically appealing, it has yet to be justified in a rigorous way.

Mie theory includes only transverse modes, and the inclusion of longitudinal modes by the theory of Ruppin[29] yields essentially no change from Mie theory for $\omega<\omega_p$ because the plasmons have energies above ω_p and are only weakly excited. The plasmon excitation is due to a nonzero value of τ. The peak in the adsorption at $\omega_p/\sqrt{3}$ is due to the excitation of surface plasmon modes of the sphere. It might appear that the enhanced yields of SSS are simply due to such an effect which occurs when $\epsilon(\omega_s)+2=0$. In a free-electron material, this condition yields $\omega_s=\omega_p/\sqrt{3}$, while in the materials used by SSS ω_s can be determined from the measured values of $\epsilon(\omega)$. It is found that the threshold energies observed by SSS do not correspond to ω_s, and consequently surface-plasmon excitation cannot explain their results.

The results for α_{I} and α_{II} shown in Fig. 1 are remarkably similar, which is encouraging in that it suggests that the results are somewhat insensitive to the particular ansatz used for the fictitious current. It is clear from the curves that there is a large enhancement with respect to the Mie result and this must be due to *e-h* —pair excitation. The enhancement is least near $\omega_p/\sqrt{3}$ where the adsorption is dominated by the transverse modes. α_{I} has a rather peculiar behavior ω_p; for this reason and owing to the difficulty discussed immediately after Eq. (5.12), we favor the adsorption given by α_{II}.

In Fig. 2, the yield of a sphere is compared to

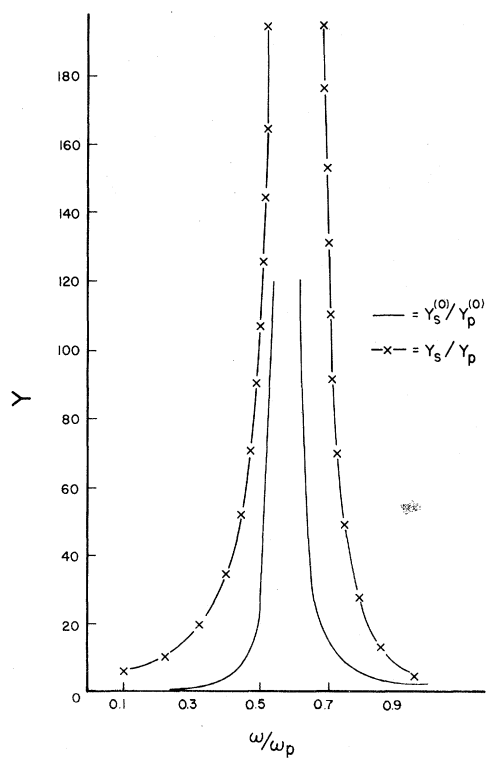

FIG. 2. Plot of the ratio of the yield of a sphere to that of a plane surface. The parameters are as in Fig. 1; also, the electron mean free path $\lambda=21.2$ Å, and for the plane the angle of incidence is $\theta=45°$. $Y_s^{(0)}/Y_p^{(0)}$ is the ratio when only transverse excitations are considered and Y_s/Y_p includes *e-h* pairs and plasmons as well.

that of a plane surface. The sphere yield is given by Eq. (5.24) in conjunction with $\alpha_{\rm II}$ while the yield of a plane surface is obtained from the theory of Kliewer.[9] SSS compared the yield of a sphere with that of a large-radius wire. There have not been any calculations of the yield for a wire so we approximate a large radius wire by a plane surface with light incident at 45° (it is not possible to average the yield of a plane over all angles because Kliewer's theory is invalid for large angles of incidence). Two curves are presented in Fig. 2; $Y_s^{(0)}/Y_p^{(0)}$ is the ratio of sphere to plane yields in the case that only transverse excitations are considered while Y_s/Y_p includes *e-h* pairs (as well as plasmons which have a negligible effect for $\omega<\omega_p$). Because SSS used unpolarized light, we use a yield for the plane that is an average of the yields for *s*- and *p*-polarized light. Again we have used $R=25$ Å, $r_s=4$, $\omega_p\tau=10^3$, and $\lambda=21.2$ Å. The calculations are relatively insensitive to all the parameters except $\omega_p\tau$, as will be discussed. The enhanced values of Y_s/Y_p compared to $Y_s^{(0)}/Y_p^{(0)}$ indicate that *e-h*—pair excitation enhances the yield of a sphere far more than they enhance the yield of a plane surface. This is directly related to the ability of the sphere to respond off resonance, i.e., away from $\omega_p/\sqrt{3}$, when *e-h*—pair excitations are taken into account combined with the fact that light cannot excite surface plasmons in the case of a plane surface.

In Fig. 3, we plot $\alpha_{\rm II}$ and $\alpha_{\rm Mie}$ for $R=25$ Å, $r_s=4$, and $\omega_p\tau=10$, 10^2, and 10^3. It is seen that $\alpha_{\rm Mie}\propto(\omega_p\tau)^{-1}$ because the absorption is due to transverse modes only. $\alpha_{\rm II}$ includes *e-h*—pair excitations and so does not scale with $(\omega_p\tau)^{-1}$. In Fig. 4 we plot $Y_p^{(0)}$ and Y_p, the yields for a plane surface not including and including *e-h*—pair excitations. The parameters chosen are again $r_s=4$, $\lambda=21.2$ Å, and $\omega_p\tau=10$, 10^2, and 10^3. $Y_p^{(0)}$ is the yield due to transverse modes only and is proportional to $(\omega_p\tau)^{-1}$ while Y_p includes *e-h*—pair excitations. Just as in the case of the sphere, the increase in the yield due to *e-h* pairs does not scale with $(\omega_p\tau)^{-1}$. The enhancements in the yields in both cases becomes quite small for $\omega_p\tau<10^2$. This is relevant because an estimate of $\omega_p\tau$ for the alkali metals as obtained from the plasmon broadening gives $\omega_p\tau<10^2$ and the effects we are concerned with would be small at least in the case for which our calculations should really apply since they make use of the free electron dielectric function. However, there are two arguments that counter such a conclusion: (i) The plasmon damping is primarily due to interband transitions which are

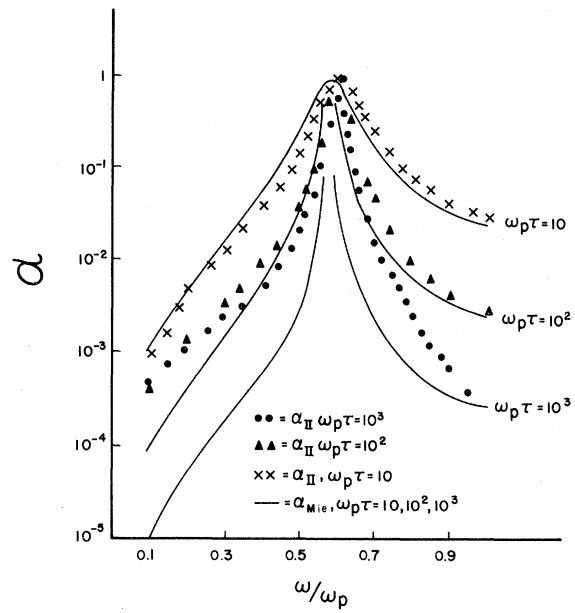

FIG. 3. Plot of $\alpha_{\rm Mie}$,$\alpha_{\rm II}$ (as in Fig. 1) for $R=25$ Å, $r_s=4$, and $\omega_p\tau=10$, 10^2, and 10^3.

not explicitly included in the dielectric function we used; i.e., there are no interband *e-h* excitations. Thus, it is inconsistent to use a value of $\omega_p\tau$ estimated from plasmon dampling without including interband adsorption in calculating the optical properties. (ii) The current theory, which represents an extension of the semiclassical infinite barrier (SCIB) approximation to the case of a sphere, has a number of strong points; it makes use

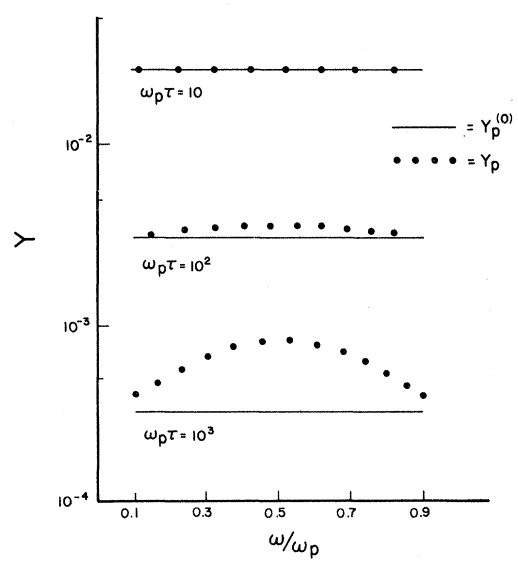

FIG. 4. Plot of $Y_p^{(0)}$ and Y_p (as in Fig. 2) for a plane surface with $r_s=4$, $\lambda=21.2$ Å and $\omega_p\tau=10$, 10^2, and 10^3.

of the bulk dielectric function, it treats transverse and longitudinal modes on an equal footing, and the physics is fairly transparent. It has the drawback that it may not be as accurate as one would wish. There is strong evidence that the theory greatly underestimates the importance of the *e-h* excitations relative to transverse ones in the optical adsorption. Calculations by Feibelman[12–15] predict a much larger contribution to the absorption due to *e-h* pairs than does the Kliewer theory (SCIB) and there is experimental evidence[4,5] favoring Feibelman. A large *e-h* —pair contribution to the optical absorption relative to the transverse mode contribution is obviously favorable to the argument that such effects are important in spheres, and by examining the ratio of Y_s to Y_p, both calculated in the SCIB approximation rather than just the magnitude of Y_s, we may be eliminating some of the error that arises from the SCIB.

In conclusion, we have extended the calculation of the surface photoelectron effect to the case of a sphere through the use of an ansatz that simulates boundary scattering by a fictitious current. We have presented numerical results for a free-electron sphere with weak scattering and we find that effect of *e-h* —pair excitations is much larger for a sphere than for a plane surface. While the results are not directly applicable to the nonfree-electron materials used by SSS, they are certainly suggestive.

Note added in proof. Very recently Apell and Ljungbert (unpublished) developed a method for the sphere that allows inclusion of *e-h* excitations without requiring the SCIB approximation; however, no numerical results are presented.

APPENDIX A

We solve for the vector potential $\vec{A}$ assuming the ansatz equation (4.1) in the case of a plane surface. Combining Eqs. (4.7a) and (4.7b) yields

$$ikk_0^2B_x+k_0^2B_z'=-[ik\gamma_x\delta(z)+\gamma_z\delta'(z)]\ , \quad \text{(A1)}$$

where B_i is defined in Eq. (4.8a).

Introducing the Fourier transforms of $\overleftrightarrow{\epsilon}^B$ and $\vec{A}$ gives

$$\begin{aligned} ikk_0^2B_x+k_0^2B_z' &= ikk_0^2[\epsilon_{xx}^B(q)A_x(p)+\epsilon_{xz}^B(q)A_z(p)] \\ &\quad +ik_0^2p[\epsilon_{zx}^B(q)A_x(p)+\epsilon_{zz}^B(q)A_z(p)]\ , \end{aligned} \quad \text{(A2)}$$

where

$$q^2=p^2+k^2=-ik\gamma_x-ip\gamma_z\ . \quad \text{(A3)}$$

The Fourier transform of Eq. (4.7b) gives

$$\begin{aligned} &-k[pA_x(p)-kA_z(p)] \\ &\quad -k_0^2[\epsilon_{zx}^B(q)A_x(p)+\epsilon_{zz}^B(q)A_z(p)]=\gamma_z\ . \end{aligned} \quad \text{(A4)}$$

The elements of the dielectric tensor are related to the transverse and longitudinal dielectric function ϵ_t and ϵ_l by[11]

$$\epsilon_{xx}^B(q)=\frac{1}{q^2}[p^2\epsilon_t(q)+k^2\epsilon_l(q)]\ , \quad \text{(A5a)}$$

$$\epsilon_{zz}^B(q)=\frac{1}{q^2}[k^2\epsilon_t(q)+p^2\epsilon_l(q)]\ , \quad \text{(A5b)}$$

$$\epsilon_{xz}^B(q)=\epsilon_{zx}^B(q)=\frac{kp}{q^2}[\epsilon_l(q)-\epsilon_t(q)]\ . \quad \text{(A5c)}$$

Use of (A5) in (A2) and (A4) and solving for A_x,A_z gives

$$\begin{aligned} A_x(p) &= \gamma_x[R^{(2)}(p)-(k/k_0)^2S^{(0)}(p)] \\ &\quad -\gamma_zk[R^{(1)}(p)+k_0^{-2}S^{(1)}(p)]\ , \end{aligned} \quad \text{(A6a)}$$

$$\begin{aligned} A_z(p) &= -\gamma_xk[R^{(1)}(p)+k_0^{-2}S^{(1)}(p)] \\ &\quad +\gamma_z[k^2R^{(0)}(p)-k_0^{-2}S^{(2)}(p)]\ , \end{aligned} \quad \text{(A6b)}$$

where

$$R^{(i)}(p)=p^i/\{q^2[q^2-k_0^2\epsilon_t(q)]\}\ , \quad \text{(A6c)}$$

$$S^{(i)}(p)=p^i/[q^2\epsilon_l(q)]\ . \quad \text{(A6d)}$$

The magnetic field is $H_y(z)=A_x'-ikA_z$ and use of (A6a) and (A6b) gives the Fourier transform of $H_y(z)$:

$$H_y(p)=i[\gamma_xp-\gamma_zk]/[q^2-k_0^2\epsilon_t(q)]\ . \quad \text{(A7)}$$

In order to apply the boundary conditions we require $A_x(z\to 0),A_z(z\to 0)$, where $A_x(z),A_y(z)$ are

$$\begin{aligned} A_x(z) &= \gamma_x[R^{(2)}(z)-(k/k_0)^2S^{(0)}(z)] \\ &\quad -\gamma_zk[R^{(1)}(z)-k_0^{-2}S^{(1)}(z)]\ , \end{aligned} \quad \text{(A8a)}$$

$$\begin{aligned} A_z(z) &= -\gamma_xk[R^{(1)}(z)-k_0^{-2}S^{(1)}(z)] \\ &\quad +\gamma_z[k^2R^{(0)}(z)-k_0^{-2}S^{(2)}(z)]\ , \end{aligned} \quad \text{(A8b)}$$

where

$$R^{(i)}(z)=\int_{-\infty}^{\infty}\frac{dp}{2\pi}e^{ipz}R^{(i)}(p)\ , \quad \text{(A8c)}$$

$$S^{(i)}(z)=\int_{-\infty}^{\infty}\frac{dp}{2\pi}e^{ipz}S^{(i)}(p)\ . \quad \text{(A8d)}$$

In the limit $z\to 0$, $R^{(i)}(z)\to 0$ since $R^{(i)}$ is an odd function of p. However, $S^{(1)}(z)\to 0$ because $S^{(1)}(p)\to p^{-1}$ for large p. This is dealt with by writing

$$S^{(1)}(z\to 0)=\int_{-\infty}^{\infty}\frac{dp}{2\pi}(p/q^2)(\epsilon_l^{-1}-1)+\int_{-\infty}^{\infty}\frac{dp}{2\pi}(p/q^2)e^{i\delta z}=i/2\ , \tag{A9}$$

where $\delta\to 0+$. Similarly,

$$S^{(0)}(z\to 0)=\int_{-\infty}^{\infty}\frac{dp}{2\pi}(1/q^2)(\epsilon_l^{-1}-1)+(1/2k)\ , \tag{A10}$$

$$S^{(2)}(z\to 0)=\int_{-\infty}^{\infty}\frac{dp}{2\pi}(p^2/q^2)(\epsilon_l^{-1}-1)-(1/2k)\ .$$

By replacing $\epsilon_t(q)$ by $\epsilon_t(0)$ in (A6c) one obtains

$$R^{(0)}(z\to 0)=\tfrac{1}{2}q_t^{-2}(-k^{-1}+ip_t^{-1})\ , \tag{A11}$$

$$R^{(2)}(z\to 0)=\tfrac{1}{2}q_t^{-2}(k+ip_t)\ , \tag{A12}$$

where

$$p_t^2=q_t^2-k^2\ , \tag{A13}$$

$$q_t^2=k_0^2\epsilon_t(0)\ . \tag{A14}$$

Similarly from (A7),

$$H_y(z\to 0)=-\tfrac{1}{2}[\gamma_x-(k/p_t)\gamma_z]\ . \tag{A15}$$

From (4.10a) and (4.10b) the fields outside the solid satisfy

$$A_x^0(z\to 0)=-(p_0/k_0)A_0(1-\rho)\ , \tag{A16}$$

$$A_z^0(z\to 0)=(k/k_0)A_0(1+\rho)\ , \tag{A17}$$

$$H_y^0(z\to 0)=-ik_0A_0(1+\rho)\ . \tag{A18}$$

Use of the boundary conditions A_z, H_y continuous now gives

$$\gamma_z=0\ , \tag{A19}$$

$$\rho A_0+(i/2k_0)\gamma_x=-A_0\ . \tag{A20}$$

Use of A_x continuous and (A19) gives

$$\rho A_0-\gamma_x(k_0/p_0)\left[\tfrac{1}{2}(k-ip_t)^{-1}-\tfrac{1}{2}(k/k_0^2)-(k/k_0)^2\int_{-\infty}^{\infty}\frac{dp}{2\pi}\frac{1}{q^2}\left[\frac{1}{\epsilon_l}-1\right]\right]=A_0 \tag{A21}$$

The result (A19) ensures that the final expressions for A_x, A_z agree with those of Ref. 11 [compare (A6a) and (A6b) with B.12 of Ref. 11].

APPENDIX B

The theorem expressed by (5.4a), (5.4b), and (5.4c) is proved by Fourier transforming the tensor product and then using an integral representation of the spherical vector functions. Here we demonstrate (5.4a), and the others follow similarly. The expression for $\vec{m}(k,\vec{r})$ given in (3.26a) can be written as[31]

$$\vec{m}(k,\vec{r})=A\int d\Omega_k(\vec{k}\times\vec{r})e^{i\vec{k}\cdot\vec{r}}Y(\Omega_k)\ , \tag{B1}$$

where $A=i^{1-l}/4\pi$ and subscripts have been dropped for simplicity. Then using the fact that $\vec{m}$ is purely transverse, we write

$$\overleftrightarrow{\epsilon}_B(\vec{r})\cdot\vec{m}(k,\vec{r})=\int\frac{d^3k'}{(2\pi)^3}e^{i\vec{k}'\cdot\vec{r}}\overleftrightarrow{\epsilon}_t(k')\cdot\vec{m}(k,\vec{k}')\ , \tag{B2}$$

where $\vec{m}(k,\vec{k}')$ is the Fourier transform of $\vec{m}(k,\vec{r})$.

With the use of (B1), the right-hand side of (B2) yields

$$A\int\frac{d^3k'}{(2\pi)^3}e^{i\vec{k}'\cdot\vec{r}}\int d^3r'e^{-i\vec{k}'\cdot\vec{r}'}\overleftrightarrow{\epsilon}_t(k')\cdot\int d\Omega_k(\vec{k}\times\vec{r}')e^{i\vec{k}\cdot\vec{r}'}Y(\Omega_k)$$
$$=iA\int d^3k'e^{i\vec{k}\cdot\vec{r}}\int d\Omega_k Y(\Omega_k)\overleftrightarrow{\epsilon}_t(k')\cdot(\vec{k}\times\vec{\nabla}_{\vec{k}'})\delta(\vec{k}'-\vec{k})\ .$$

Now integrate by parts to get

$$A\int\frac{d^3k'}{(2\pi)^3}e^{i\vec{k}'\cdot\vec{r}}\int d^3r'e^{-i\vec{k}'\cdot\vec{r}'}\overleftrightarrow{\epsilon}_t(k')\cdot\int d\Omega_k(\vec{k}\times\vec{r}')e^{i\vec{k}\cdot\vec{r}'}Y(\Omega_k)$$
$$=-iA\int d\Omega_k Y(\Omega_k)\overleftrightarrow{\epsilon}_t(k)\cdot(\vec{k}\times\vec{\nabla}_{\vec{k}})e^{i\vec{k}\cdot\vec{r}}$$
$$=A\int d\Omega_k Y(\Omega_k)\overleftrightarrow{\epsilon}_t(k)\cdot(\vec{k}\times\vec{r})e^{i\vec{k}\cdot\vec{r}}$$
$$=\overleftrightarrow{\epsilon}(k)\cdot\vec{m}(k,\vec{r})\ . \tag{B3}$$

APPENDIX C

Equation (5.5) is derived. Use of (5.1), (5.3), and (5.4) in (4.1) gives

$$\sum_i \int dk\,[(k^2-k_0^2\epsilon_t)(a_i\vec{m}_i+b_i\vec{n}_i)-k_0^2\epsilon_l c_i\vec{1}_i]=\frac{4\pi}{c}\delta(r-R)\sum_i(\alpha_i\gamma_i\hat{r}+\beta_i\vec{L}Y_i+\gamma_i\hat{r}\times\vec{L}Y_i)\ , \tag{C1}$$

where i stands for an appropriate set of quantum numbers. Taking the divergence of both sides of (C1) and using the fact that $\vec{\nabla}\cdot\vec{m}=\vec{\nabla}\cdot\vec{n}=0$ gives

$$k_0^2\sum_i\int dk\,k^2\epsilon_l c_i j_i(kr)Y_i=\frac{4\pi}{c}\sum_i\left[\alpha_i\frac{1}{r^2}\frac{\partial}{\partial r}r^2\delta(r-R)Y_i-i\gamma_i i(i+1)\frac{\delta(r-R)}{R}Y_i\right]\ , \tag{C2}$$

Equation (C2) yields

$$c_i=-\frac{8Rc}{\omega^2}[\alpha_i kRj_i'(kR)+i\gamma_i(i+1)j_i(kR)]\ . \tag{C3}$$

Use of Eq. (3.26) in (C1) and a comparison of the terms proportional to $\vec{L}Y_i$ gives

$$-i\int dk(k^2-k_0^2\epsilon_t)a_i j_i(kr)=\frac{4\pi}{c}\delta(r-R)\beta_i\ , \tag{C4}$$

which gives

$$a_i=i\,8\frac{(kR)^2}{c}\beta_i\frac{j_i(kR)}{k^2-k_0^2\epsilon_t}\ . \tag{C5}$$

Use of (C5) in (C1) yields

$$\sum_i\int dk[(k^2-k_0^2\epsilon_t)b_i\vec{n}_i-k_0^2\epsilon_l c_i\vec{1}_i]=\frac{4\pi}{c}\delta(r-R)\sum_i(\alpha_i Y_i\hat{r}+\gamma_i\hat{r}\times\vec{L}Y_i)\ . \tag{C6}$$

Taking the curl of both sides of (C6) gives

$$-i\sum_i\int dk\,k(k^2-k_0^2\epsilon_t)b_i j_i(kr)\vec{L}Y_i=\frac{4\pi}{c}\sum_i\left[-i\alpha_i\frac{\delta(r-R)}{R}\vec{L}Y_i-\gamma_i\frac{1}{r}\frac{\partial}{\partial r}r\delta(r-R)\vec{L}Y_i\right]\ . \tag{C7}$$

Equation (C7) yields

$$b_i=\frac{8}{c}\frac{kR}{k^2-k_0^2\epsilon_t}\{\alpha_i j_i(kr)+i\gamma_i[kRj_i(kR)]'\}\ . \tag{C8}$$

APPENDIX D

The use of (5.5) in (5.1) and then application of the boundary conditions on the surface of the sphere yield a number of integrals over wave vectors that involve the dielectric functions and products of Bessel functions. We point out some pitfalls involved in evaluating these integrals on the surface of the sphere and illustrate these with some typical examples.

The field coefficients $a_l(k)$, $b_l(k)$, and $c_l(k)$ in (5.5) involve Bessel functions evaluated at the surface $r=R$ because of the nature of the current in (5.3). When (5.5) is used in (5.1), we obtain an expression for the fields inside the sphere, $r\le R$. Application of the boundary conditions requires that r approach R from below. In this limit it is necessary to differentiate between integrals such as

$$I_a(g)=\int_0^\infty dk\,g(k)j_l(kR^>)kR^< j_l'(kR^<) \tag{D1}$$

and

$$I_b(g)=\int_0^\infty dk\,g(k)j_l(kR^<)kR^> j_l'(kR^>)\ , \tag{D2}$$

where $R^{>}=R+\delta$, $R^{<}=R-\delta$, and $g(k)$ is an even function of k. If $g(k)$ does not approach zero as $k\to\infty$, it is possible for I_a and I_b to have different values in the limit $\delta\to 0$. This can be seen in the example $g(k)=1$ by evaluating I_a and I_b by contours. The convergence of the integrands on the piece of the contours at infinity is controlled by the Bessel function with argument $kR^{>}$. Thus we can divide (B1) into two integrals using $j_l(kR^{>})=\frac{1}{2}[h_l^{(1)}(kR^{>})+h_l^{(2)}(kR^{>})]$, and (B2) into two integrals using $j_l'(kR^{>})=\frac{1}{2}[h_l^{(1)'}(kR^{>})+h_l^{(2)'}(kR^{>})]$. The contours involving $h_l^{(1)}$ can then be closed in the upper half-plane and those involving $h_l^{(2)}$ can be closed in the lower half-plane. However, since the convergence of I_a and I_b is controlled by different functions, i.e., $h_l^{(1)}$ and $h_l^{(1)'}$, the residues at $k=0$ also differ. We find

$$I_a(1)=\frac{\pi}{2(2l+1)}l\frac{R^{<l}}{R^{>l+1}}\,, \tag{D3}$$

$$I_b(1)=-\frac{\pi}{2(2l+1)}(l+1)\frac{R^{<l+1}}{R^{>l+2}}\,, \tag{D4}$$

which differ by $\pi/2R$ as $\delta\to 0$.

This difference arising from the behavior of the integrand at infinity is eliminated if $g(k)$ itself approaches zero as $k\to\infty$. When ϵ_T is approximated as a local function, typical integrals which result are given by $g(k)=(k^2-k_T^2)^{-1}$ in (D1) and (D2) $[k_t^2=k_0^2\epsilon_t(0)]$. When the contours are performed as above we find

$$I_a((k^2-k_t^2)^{-1})=\frac{i\pi}{2k_t}j_l'(k_tR^{<})k_tR^{<}h_l^{(1)}(k_tR^{>})-\frac{\pi}{2k_t}\frac{l}{2l+1}\frac{1}{k_tR}\,, \tag{D5}$$

$$I_b((k^2-k_t^2)^{-1})=\frac{i\pi}{2k_t}j_l(k_tR^{<})k_tR^{>}h_l^{(1)'}(k_tR^{>})+\frac{\pi}{2k_t}\frac{l+1}{2l+1}\frac{1}{k_tR}\,. \tag{D6}$$

These are seen to be identical in the limit $\delta\to 0$ when we use $j_l(x)h_l^{(1)'}(x)-j_l'(x)h_l^{(1)}(x)=i/x^2$. The pole structure of $g(k)$ and the $k=0$ poles combine to give the same result in each case.

Other integrals which arise are those involving the longitudinal dielectric function such as $g(k)=\epsilon_l^{-1}(k)$ in (D1) and (D2). These integrals we have chosen to evaluate numerically. However, since $\epsilon_l(k)\to 1$ as $k\to\infty$, ambiguities similar to (D3) and (D4) present a problem for numerical evaluation. This can be overcome by adding and subtracting 1 from the integrand. We then have a well-defined integral with $g(k)=\epsilon_l^{-1}(k)-1$ which can be calculated numerically in a straightforward manner. The remaining pieces can be evaluated analytically by contours, in this example yielding (D3) and (D4).

APPENDIX E

We present the integrals over solid angle involving the spherical vector functions which are necessary to calculate the small-particle absorption as given by (5.2). Integrals between functions of opposite parity vanish identically. The nonvanishing integrals are as follows:

$$\int_R d\Omega\,\hat{r}\cdot(\vec{m}_{o1l}\times\vec{n}_{o1l'}^{*})=j_l(k_tR)\left[\frac{[k_tRj_l(k_tR)]'}{k_tR}\right]^{*}\frac{2\pi}{2l+1}l^2(l+1)^2\delta_{ll'}\,, \tag{E1}$$

$$\int_R d\Omega\,\hat{r}\cdot(\vec{n}_{e1l}\times\vec{m}_{e1l}^{*})=-j_l^{*}(k_tR)\left[\frac{[k_tRj_l(k_tR)]'}{k_tR}\right]\frac{2\pi}{2l+1}l^2(l+1)^2\delta_{ll'}\,, \tag{E2}$$

$$\int_R d\Omega\,\hat{r}\cdot(\vec{l}_{e1l}\times\vec{m}_{e1l'}^{*})=-\frac{1}{R}j_l(kR)j_l^{*}(k_tR)\frac{2\pi}{2l+1}l^2(l+1)^2\delta_{ll'}\,. \tag{E3}$$

Here $\vec{m}=\vec{m}(k_t,\vec{r})$, $\vec{n}=\vec{n}(k_t,\vec{r})$, and $\vec{l}=\vec{l}(k,\vec{r})$.

APPENDIX F

In this appendix, we derive an expression for the absorption assuming that there are no e-h —pair excitations, but that plasmons can be excited. Thus we evaluate Eq. (5.8) for the case that

$$\epsilon_l(q)=\epsilon_{\rm pl}(q)\equiv 1-\frac{\omega_p^2}{\omega^2-\alpha q^2-i\omega/\tau} . \tag{F1}$$

In order to evaluate (5.8), we require Δ_l of (5.7e) and consequently the $Q_l^{(i)}$ of Eq. (5.7g). These integrals can be done by contour integration as is demonstrated for $Q_l^{(1)}$,

$$Q_l^{(1)}=R\int_0^\infty dq(\epsilon_{\rm pl}^{-1}-1)j_l(qR)^2=\lim_{R^<\to R^>\to R}(1/2R)\int_{-\infty}^{\infty}dq(\epsilon_{\rm pl}^{-1}-1)j_l(qR^<)j_l(qR^>) . \tag{F2}$$

$Q_l^{(1)}$ now has the same form as the integrals discussed in Appendix D, the term $j_l(qR^>)$ is split into terms proportional to $e^{iqR^>}$ and $e^{-iqR^<}$, and the correspnding contours are closed in the upper- and lower-half planes. There is then a contribution from the pole at $q=0$ from the plasmon wave vector $q_{\rm pl}$

$$\epsilon_{\rm pl}(q_{\rm pl})=0 , \tag{F3}$$

where $q_{\rm pl}$ will in general be complex. One obtains

$$Q_l^{(1)}=\frac{\pi}{2(2l+1)}\left[\frac{1}{\epsilon_{\rm pl}(0)}-1\right]+\gamma j_l(\rho_0)h_l(\rho_o) , \tag{F4a}$$

$$Q_l^{(2)}=\gamma j_l(\rho_0)\rho_0 h_{l-1}(\rho_0) \tag{F4b}$$

$$=\frac{\pi}{2}\left[\frac{1}{\epsilon_{\rm pl}(0)}-1\right]+\gamma\rho_0 j_{l-1}(\rho_0)h_l(\rho_0) , \tag{F4c}$$

$$Q_l^{(3)}=\gamma\rho_0 j_{l-1}(\rho_0)\rho_0 h_{l-1}(\rho_0) , \tag{F4d}$$

where

$$\rho_0=q_{\rm pl}R , \tag{F4e}$$

$$\gamma=\frac{2\pi iR}{\left|\frac{\partial\epsilon}{\partial q}\right|_{q_{\rm pl}}} , \tag{F4f}$$

where h_l is the Hankel function of the first kind. The two different expressions for $Q_l^{(2)}$, Eqs. (F4b) and (F4c) result from replacing $j_{l-1}(qR)j_l(qR)$ by $j_{l-1}(qR^<)j_l(qR^>)$ or by $j_{l-1}(qR^>)j_l(qR^<)$ in Eq. (5.6g). Use of Eq. (F4) in Eq. (5.6e) gives

$$\Delta_l=-\frac{\pi}{2}\left[\frac{l+1}{2l+1}\right]\left[\frac{1}{\epsilon_{\rm pl}(0)}-1\right]\times\frac{\rho_0 j_{l-1}(\rho_0)-(2l+1)j_l(\rho_0)}{\rho_0 j_l(\rho_0)'} . \tag{F5}$$

*Present address: Naval Research Laboratory, Washington, D. C. 20375.

[1]M. Anderegg, B. Feuerbacher, and B. Fitton, Phys. Rev. Lett. 27, 1565 (1971).
[2]J. K. Sass, H. Laucht, and K. L. Kliewer, Phys. Rev. Lett. 35, 1461 (1975).
[3]H. Peterson and S. B. M. Hagstrom, Phys. Rev. Lett. 41, 1314 (1978).
[4]H. J. Levinson, E. W. Plummer, and P. J. Feibelman, Phys. Rev. Lett. 43, 952 (1979).
[5]Guy Jezequel, Phys. Rev. Lett. 45, 1963 (1980).
[6]K. L. Kliewer and R. Fuchs, Phys. Rev. Lett. 172, 607 (1968).
[7]R. Fuchs and K. L. Kliewer, Phys. Rev. Lett. 185, 905 (1969).
[8]K. L. Kliewer, Phys. Rev. Lett. 33, 900 (1974).
[9]K. L. Kliewer, Phys. Rev. B 14, 1412 (1976).
[10]K. L. Kliewer, Phys, Rev. B 15, 3759 (1977).
[11]G. Mukhopadhyay and S. Lundquist, Phys. Scr. 17, 69 (1978).
[12]P. J. Feibelman, Phys. Rev. Lett. 34, 1092 (1975).
[13]P. J. Feibelman, Phys. Rev. B 12, 1319 (1975).
[14]P. J. Feibelman, Phys. Rev. B 12, 4282 (1975).
[15]P. J. Feibelman, Phys. Rev. B 14, 762 (1976).
[16]A. R. Melnyk and M. J. Harrison, Phys. Rev. B 2, 835 (1970).
[17]B. B. Dasgupta and R. Fuchs, Phys. Rev. B 24, 554 (1981).
[18]S. Twamey, *Atmospheric Aerosols* (Elsevier, Amsterdam, 1977).
[19]B. J. Finlayson-Pitts and J. N. Pitts. Jr., in *Advances in Environmental Science and Technology,* edited by J. N. Pitts. Jr. and R. L. Metcalf (Wiley, New York, 1977), Vol. 7, p. 75.
[20]T. Novakov, S. G. Chang, and A. B. Harker, Science 186, 259 (1974).

[21]A. Schmidt-Ott, P. Schurtenberger, and H. C. Siegmann, Phys. Rev. Lett. 45, 1284 (1980).
[22]A. A. Lushnikov and A. J. Simonov, Phys. Lett. 44A, 45 (1973).
[23]M. J. Rice, W. R. Schneider, and S. Strassler, Phys. Rev. B 8, 474 (1973).
[24]R. H. Ritchie and A. L. Marusak, Surf. Sci. 4, 234 (1966).
[25]J. Crowell and R. H. Ritchie, Phys. Rev. 172, 436 (1968).
[26]P. Ascarelli and M. Cini, Solid State Commun. 18, 385 (1976).
[27]B. B. Dasgupta. Z. Phys. B 27, 75 (1977).
[28]B. B. Dasgupta and R. Fuchs, Phys. Rev. B 24, 554 (1981).
[29]R. Ruppin, Phys. Rev. B 11, 2871 (1975).
[30]G. Mie, Ann. Phys. (Leipzi) 25, 377 (1908).
[31]David R. Penn and R. W. Rendell, Phys. Rev. Lett. 47, 1067 (1981).
[32]J. A. Stratton, *Electro-magnetic Theory* (McGraw-Hill, New York, 1941), p. 414.
[33]J. Lindhard, K. Dansk. Vidensk. Selsk. Mat-Fys. Medd. 28, No. 8 (1954).
[34]Reference 11 is a microscopic derivation of the results of Ref. 6. There are, however, some errors in Ref. 11 and the authors incorrectly conclude that $\vec{E}_\perp$ is not continuous.
[35]N. D. Mermin, Phys. Rev. B 1, 2362 (1970).
[36]A. Kawabata and R. Kuba, J. Phys. Soc. Jpn. 21, 1765 (1966); U. Kreibig, J. Phys. F 4, 999 (1974); R. Ruppin and Y. Yatom, Phys. Status Solidi B 74, 647 (1976).